Probability distributions of monthly-to-annual mean temperature and precipitation in a changing climate (CES Climate Modelling and Scenarios Deliverable D2.4, task I)

Jouni Räisänen
Department of Physics, P.O. Box 48, FI-00014 University of Helsinki, Finland
Email: jouni.raisanen@helsinki.fi

17 November 2009

AVAILABLE FROM:
http://www.atm.helsinki.fi/~jaraisan/CES_D2.4/CES_D2.4_task1.html

Table of Contents

Abstract **1**
1. Introduction **2**
2. Methods and data sets **5**
3. Results for temperature **7**
4. Results for precipitation **14**
5. Tables for individual locations **19**
6. Summary **24**
Appendix: details of methodology **26**
A.1 Data sets 26
A.2 Derivation of regression coefficients 27
A.3 Smoothing of the probability distributions 30
References **31**

Abstract

The operational description of climate has been traditionally based on past observations, using a 30-year normal period such as 1961-1990. In a world with ongoing anthropogenic climate change, however, past data give a potentially biased estimate of the actual present-day and near-future climate. Here we attempt to correct this bias with a “delta change” method, in which model-simulated climate changes and observed global mean temperature changes are used to extrapolate past observations forward in time, to make them representative of present or future climate conditions. By using this method, we estimate the probability distributions that characterize the interannual variability of temperature and precipitation in the present (year 2010) climate and later, up to the year 2050, assuming best-estimate climate changes under the SRES A1B emission scenario.

Changes in temperature are likely to proceed much faster in comparison with natural variability than those in precipitation. At present (2010), typically about 70% of all months are expected to be warm (above the median for 1961-1990) in northern Europe, and by the year 2050 this fraction is projected to approach 90%. The impact of anthropogenic climate change on precipitation is still estimated to be very small at present. In the middle of this century, typically about 60% of all months are projected to have above-median precipitation in northern Europe, although with a substantial variation with the time of the year.

An on-line appendix of this report provides detailed tables of the estimated probability distributions of temperature and precipitation variability as a function of time, up to the year 2050, at 120 Nordic locations for temperature and at 230 locations for precipitation.

1. Introduction

Weather services base their operational definition of climate on past observations. Commonly, a 30-year normal period such as 1961-1990 is used (World Meteorological Organization (WMO) 1989). However, in a world with ongoing, presumably largely anthropogenic climate change (Hegerl et al. 2007), past statistics give a potentially biased estimate of the present and near-future climate. This is not only the case for time mean conditions (e.g., the long-term mean temperature), but also for many other aspects of climate variability (e.g., the frequency of “very warm” months exceeding a given threshold temperature).

On the other hand, the natural interannual variability of climate in northern Europe is substantial. Given this background of variability, are the effects of climate change large enough to be of practical importance in the near future?

This report aims to address the impact of climate change on present and near-future climate in northern Europe. As a first illustration, Fig. 1.1 shows alternative probability distributions of December mean temperature for Helsinki, Finland. The first one (blue line) is estimated directly from the observations for 1961-1990, the official WMO normal period. The second one (in green), was obtained by extending the observational baseline by 18 years, up to the year 2008. This should yield a better estimate of the present climate than the data for 1961-1990 alone, both because the increase in sample size reduces sampling uncertainty and because later observations are more representative of current climatic conditions. Because many mild Decembers occurred in 1991-2008, the distribution for 1961-2008 has shifted to the right (i.e., towards higher temperatures) from that for 1961-1990.

Nevertheless, the ongoing global climate change implies that even the distribution for 1961-2008 gives a biased estimate for the currently prevailing climate. This bias could be reduced by moving the beginning of the baseline period later in time, but at the cost of larger sampling uncertainty. A more appealing alternative is to take climate change into account explicitly. Here we use a method developed by Räisänen and Ruokolainen (2008a,b) for this purpose; more details are provided in Section 2 and in the appendices of this report. The resulting best-estimate distribution for the year 2010 (red line) shows a higher probability of mild Decembers, and a lower probability of cold Decembers, than either of the two directly observation-based distributions. This estimate is based partly on climate model results and is therefore potentially affected by modelling uncertainty. To illustrate this uncertainty, the thin grey lines in Fig. 1.1 show the distributions obtained when using 19 climate models individually. Although the magnitude of the warming varies between the models, the general shift towards higher temperatures is robust.

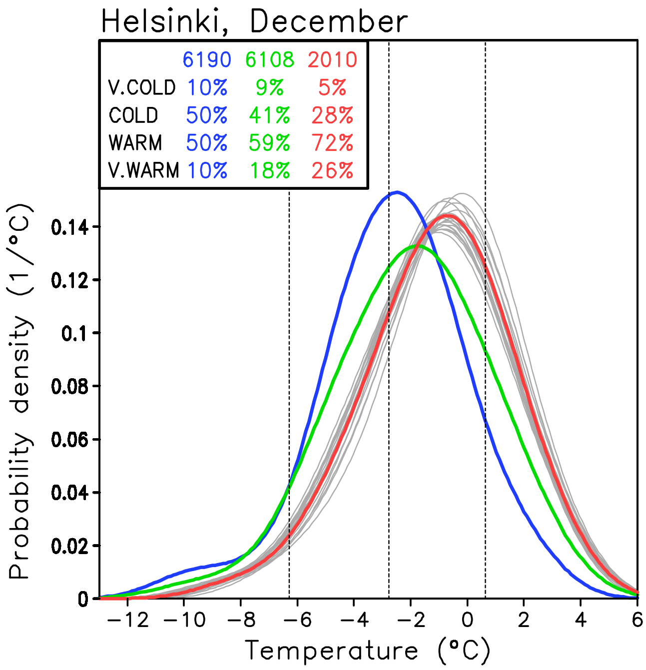

Figure 1.1. *Probability distributions of December mean temperature in Helsinki, Finland. The blue and red lines represent the distributions derived from observations for 1961-1990 and 1961-2008, respectively, using Gaussian kernel smoothing. The red line is the best model-based estimate for the distribution around the year 2010, and the thin grey lines illustrate the uncertainty associated with the choice among 19 global climate models. The numbers in the top left corner give the probabilities of very cold (below the 10th percentile in 1961-1990, threshold shown by the first vertical line), cold (below the 50th percentile, second vertical line), warm (above the 50th percentile) and very warm (above the 90th percentile, third vertical line) Decembers for 1961-1990, 1961-2008 and 2010.*

To quantify the shifts in the probability distributions, Fig. 1.1 divides December mean temperatures to four classes based on the distribution observed in 1961-1990: “very cold” (below the 10th percentile in 1961-1990), “cold” and “warm” (below and above the median), and “very warm” (above the 90th percentile). By definition, the probabilities of these classes in 1961-1990 were 10%, 50%, 50% and 10%, respectively. For the best-estimate distribution representing the year 2010, the probability of warm Decembers has increased to 72% and the probability of very warm Decembers to 26%[1]; conversely the probabilities of cold and very cold Decembers have been reduced. A part of these changes is already visible in the observed distribution for 1961-2008.

[1] In Figure 1.1, probability is proportional to area. Thus, for example, the probability of a very warm December in 2010 is obtained by integrating the area to the right of the rightmost vertical line (representing the 90th percentile in 1961-1990) and below the red curve.

Table 1.1. *Probability distributions of December mean temperature in Helsinki, Finland. The first seven columns give the 5^th^, 10^th^, 25^th^, 50^th^, 75^th^, 90^th^ and the 95^th^ percentiles of the observed distributions for the periods 1961-1990 (6190) and 1961-2008 (6108) and the model-adjusted distributions for the years 2010, 2030 and 2050. The values are multiplied by 10 (e.g. "-78" means -7.8°C). The last four columns give the probabilities of very cold (VC), cold (C), warm (W) and very warm (VW) Decembers, using threshold temperatures defined by the 10^th^, 50^th^ and 90^th^ percentiles of the distribution in 1961-1990.*

Helsinki, December

	5%	10%	25%	50%	75%	90%	95%	VC	C	W	VW
6190	−78	−63	−45	−28	−10	6	17	10	50	50	10
6108	−73	−61	−42	−21	−1	17	26	9	41	59	18
2010	−62	−50	−30	−11	7	23	32	5	28	72	26
2030	−50	−38	−19	−0	17	32	41	2	17	83	40
2050	−33	−22	−4	13	30	44	52	1	7	93	61

Some more detailed results for this case are given in Table 1.1. Shown in the table are seven percentile points of December mean temperature from 5% to 95%, together with the probabilities of very cold, cold, warm and very warm Decembers (as defined above). In addition to the three periods included in Fig. 1.1., the table also provides model-based best estimates for the distributions for the years 2030 and 2050, assuming that greenhouse gas concentrations follow the SRES A1B scenario (Nakićenović and Swart 2000). The analysis indicates that warm (cold) Decembers will become increasingly more (less) common with time. For example, the median December mean temperature in Helsinki is projected to increase to 0°C by the year 2030, whereas only one December out of ten at that time is projected to have a mean temperature colder than -3.8°C.

In the on-line appendices of this report, tables similar to Table 1.1 are provided for many more locations in the Nordic area. Both temperature and precipitation are included. In addition to the 12 calendar months, seasonal (December-February, March-May, June-August and September-November) and annual mean values are studied.

In this main report, we will first describe the methods, assumptions and data sets used in the analysis (Section 2 and Appendix). Then, an overview of the results for temperature (Section 3) and precipitation (Section 4) is provided. The set of stations for which detailed tables have been prepared is introduced in Section 5. A summary is given in Section 6.

2. Methods and data sets

When estimating the probability distributions that describe the present-day or future temperature and precipitation variability, we combine observations of the local climate with the observed evolution of the global mean temperature and model-based estimates of the geographical distribution of anthropogenic climate changes, largely following Räisänen and Ruokolainen (2008a,b). The main features of this procedure are as follows:

- Model simulations of 20^{th} and 21^{st} century climate change are used to develop linear regression equations that relate the local temperature or precipitation climate to a smoothed (11-year running mean) evolution of the global mean temperature. Two coefficients are derived for each variable. The first gives the change in the local time mean climate, and the second the per cent change in the magnitude of interannual variability per 1°C of global temperature change. This method assumes that forced changes in local climate are primarily conditioned by the change in the global mean temperature, regardless of the mechanisms that cause the global mean temperature change; the validity of this assumption is discussed in Räisänen and Ruokolainen (2006, 2008a). In contrast to Räisänen and Ruokolainen (2008a,b), who derived the regression coeffcients entirely from global climate model simulations, some information from higher-resolution regional climate models is also used here (Appendix A.2).
- The model-based regression coefficients are combined with the observed time series of the global mean temperature to extrapolate past observations forward in time. For the near-present period and for the future, for which the observed 11-year running mean global mean temperature is not yet available, this is substituted by the corresponding 11-year mean from simulations following the SRES A1B emission scenario. The emission scenario uncertainty, which is expected to remain small for the next few decades (e.g., Räisänen and Ruosteenoja 2008), is not considered here.
- By collecting all the extrapolated observations from the selected baseline period (here, we will mainly use the years 1961-2008), one obtains the sample from which the climate in the selected target year (e.g., 2010) is estimated.
- Finally, Gaussian kernel smoothing (Equation (10) in Räisänen and Ruokolainen 2008a) is applied to convert the discrete frequency distribution of the extrapolated observations to a continuous probability distribution.

The data sets used, the derivation of the regression coefficients and the Gaussian kernel smoothing are discussed in Appendices A.1-A.3. The extrapolation (or adjustment) of past observations is illustrated in Fig. 2.1, using again December mean temperature in Helsinki as an example. Each temperature or precipitation observation during the selected baseline period is replaced by a new observation, using the model-based regression coefficients and the change in the 11-year mean global mean temperature between the year of the observation and the selected target year (in Fig. 2.1, 2010). Mirroring the changes in the global mean temperature, the differences between the original and the new observations increase backward in time. However, these differences also depend on the original observations themselves, because the method takes into account model-simulated changes in interannual variability. For December mean temperature in southern Finland, the models suggest a slight decrease in variability with increasing global mean temperature. As a result, slightly smaller extrapolation increments are applied to the temperatures in mild (e.g., 1972 and 1974) than cold (e.g. 1978) Decembers.

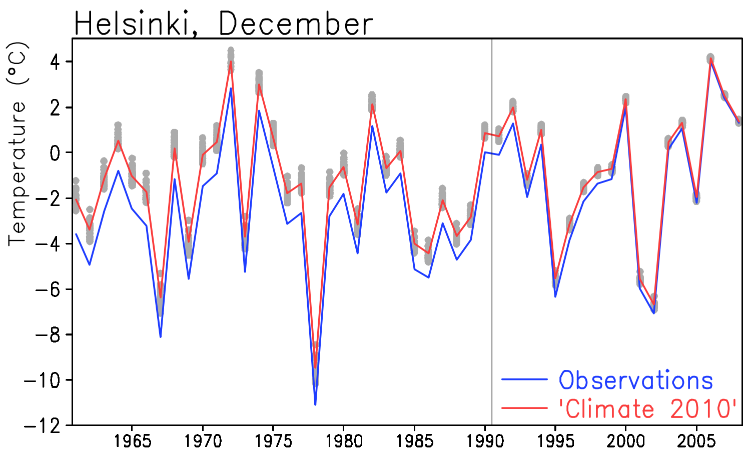

Figure 2.1. *December mean temperatures in Helsinki. The blue line shows the temperatures observed in 1961-2008, and the red line the best-estimate extrapolated temperatures representing the climate in the year 2010. The variation of the extrapolated temperatures between 19 climate models is indicated by grey dots. The end of the period 1961-1990 used for defining the observed baseline climate is shown by a vertical line.*

The extrapolation of past observations cannot be made exactly. As shown by the grey dots in Fig. 2.1, the results depend on the climate model used. The uncertainty implied by these differences increases backward in time, when the global mean temperature was further below its present-day level than in more recent years. As a result, it is not necessarily best to use all available observations when estimating the present-day (or future) climate, although this would minimize the uncertainty associated with the limited sample size. Here, we use observations from the 48-year period 1961-2008, although, for many stations, longer time series would be available. This choice is guided by the findings of Räisänen and Ruokolainen (2008a). When studying the capability of the extrapolation method to hindcast the temperatures observed in global land areas in the years 1991-2002, they found a better agreement with the observations when using a 30-year (1961-1990) than a 90-year (1901-1990) baseline period. However, for studying the frequency of extremes, a longer baseline might be preferable (Räisänen and Ruokolainen 2008b).

In the CES annual meeting in May 2009, it was recommended that climate changes should be expressed relative to the climate during the official WMO normal period 1961-1990. Therefore, the probabilities of cold, warm, dry and wet months, seasons and years are here given using threshold values derived from the observations in 1961-1990 (Table 2.1). Thus, two baselines are used for different purposes: 1961-2008 as the basis of the probability distributions that characterize the present or future climate, and 1961-1990 for putting these distributions in the context of the past. A disadvantage of this distinction is that it makes some of the present results more complicated to interpret.

As shown by Figs. 1.1 and 2.1, the estimates of current and future climate are to some extent dependent on the model used for extrapolating the observations. For brevity (and to avoid discussing the difficult concept of “probability distribution of probability distribution”), however, we focus in this report on multi-model mean (i.e., “best-estimate”) climate projections, as represented by the red lines in the mentioned two figures.

Table 2.1. *Definitions used in classifying monthly-to-annual values of temperature and precipitation.*

Very cold	Temperature below the 10^{th} percentile in 1961-1990
Cold	Temperature below the 50^{th} percentile in 1961-1990
Warm	Temperature above the 50^{th} percentile in 1961-1990
Very warm	Temperature above the 90^{th} percentile in 1961-1990
Very dry	Precipitation below the 10^{th} percentile in 1961-1990
Dry	Precipitation below the 50^{th} percentile in 1961-1990
Wet	Precipitation above the 50^{th} percentile in 1961-1990
Very wet	Precipitation above the 90^{th} percentile in 1961-1990

3. Results for temperature

Again, it is useful to start with a detailed analysis for one location (for this purpose, Helsinki will be used throughout this report). Figure 3.1 is a repetition of Fig. 1.1 for all 12 months, although excluding the year 2010 results for the individual models. At least the following main features can be seen:

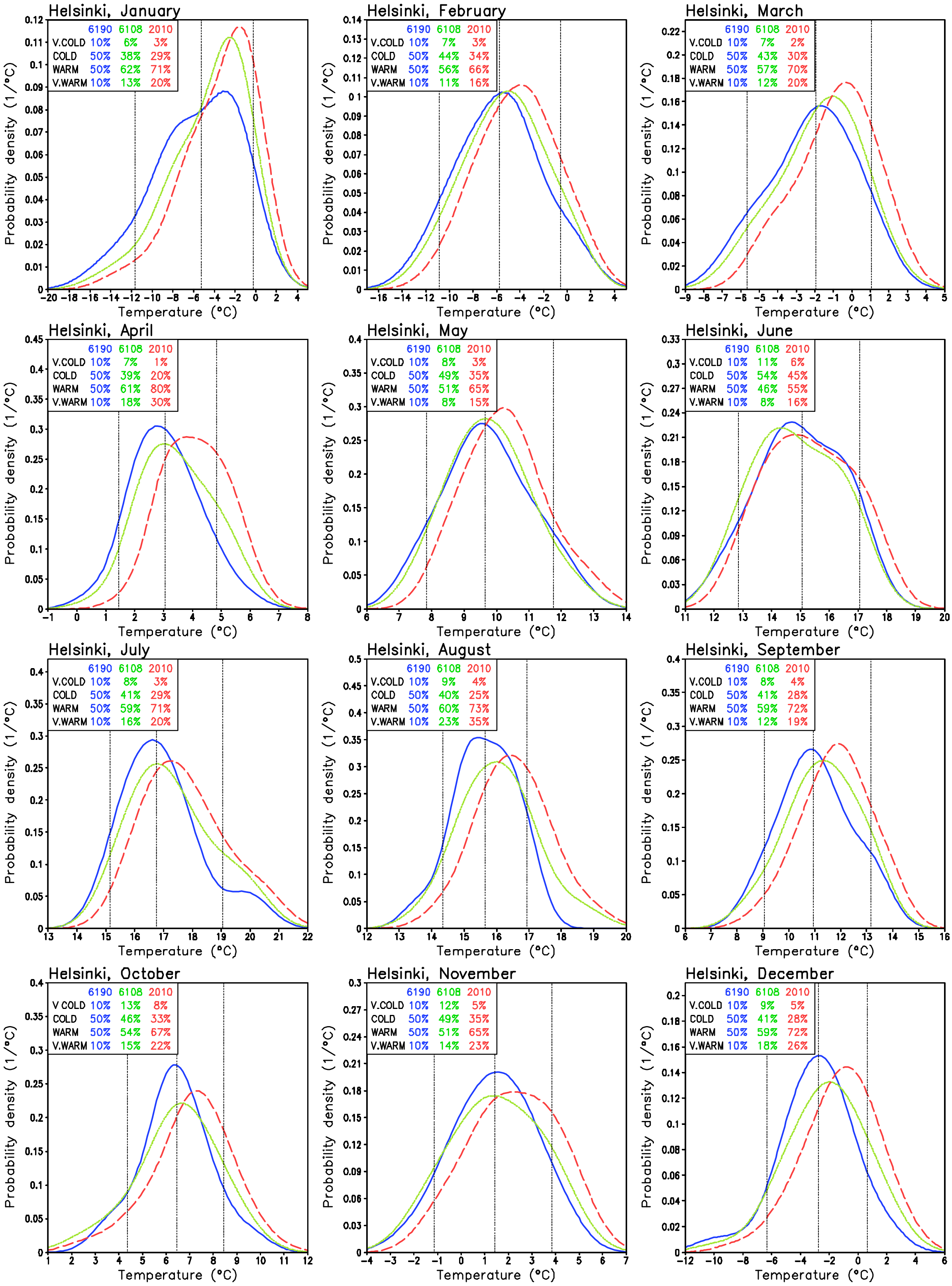

Figure 3.1. *Probability distributions of monthly mean temperature in Helsinki, Finland. The blue and the green lines represent the observations for 1961-1990 and 1961-2008, respectively, and the red lines the best-estimate distributions corresponding to the climate in the year 2010. The numbers in the top left corner give the probabilities of very cold, cold, warm and very warm months, using threshold temperatures shown by the three vertical lines. The horizontal and vertical scales vary from month to month.*

- Comparing the distributions derived from observations for 1961-1990 and 1961-2008, it is clear that the latter period was generally warmer (or, more precisely, the years 1991-2008 were warmer than 1961-1990). However, the difference varies from month to month. A marked outlier is June, with slightly lower temperatures in 1961-2008 than in 1961-1990. These month-to-month differences are likely to reflect both the effects of natural variability and genuine differences in the warming induced by changing atmospheric composition. Although the latter factor is not negligible (climate models suggest that greenhouse-gas-induced warming in northern Europe should be about twice as large in winter than in summer, see Appendix A.2), the former may be even more important.
- The difference between the model-based "2010" distribution and the observed distribution in 1961-2008 (which the "2010" distribution is built on) is invariably towards higher temperatures in 2010. This is simply because the signal of greenhouse-gas-induced climate change, as derived from the model simulations, is one with higher temperatures in all months of the year.
- Interannual temperature variability is much larger in mid-winter than in the summer half-year. As a result, the fraction of (for example) warm months is much less sensitive to changes in mean temperature in winter than in the other seasons. For example, in April the projection for 2010 suggests a 19% larger frequency of warm months than was observed in 1961-2008 (80% vs. 61%), whereas the difference in January is only 9% (71% vs. 62%). In absolute terms, however, the projected warming is larger in January than in April. Note that Fig. 3.1 hides the latter difference, because the horizontal axis is scaled according to the range of interannual variability.
- The two observation-based distributions (1961-1990 and 1961-2008) differ in some months substantially in width and shape. For example, the large differences in January are due to a complete lack of very cold Januaries after 1990 and the simultaneous occurrence of many mild Januaries. This illustrates the difficulty of estimating higher-order statistical properties of climate, such as the magnitude and distribution of variability, from small samples. In any case, 48 years is better from the sampling point of view than 30.
- Apart from the shift toward higher temperatures, the projected distributions for 2010 are similar to the observed distributions for 1961-2008. Still, a slight narrowing of the distributions is evident in most months, particularly in the winter half-year. This is partly because the models suggest a decrease in the variability of winter temperatures with increasing global mean temperature (Fig. A2.1 in Appendix A.2). In addition, the width of the 1961-2008 distributions is slightly amplified by the warming trend observed during this period in most months. When the observations are extrapolated to

the present, such warming trends are reduced or eliminated (Fig. 2.2). This also acts to narrow the distributions.

Figure 3.2 shows the calculated probability of warm (above the 50th percentile in 1961-1990) months in 2010 in map format. The probability varies on both sides of 70%, but with substantial differences from month to month and across Europe. As indicated above, these differences are affected by three factors: (i) the differences in observed temperature climate between the periods 1961-1990 and 1961-2008 (or 1991-2008), (ii) the magnitude of warming from 1961-2008 to 2010 as derived from the model simulations, and (iii) the magnitude of interannual variability. A particularly high probability of warm months, locally up to 90%, is calculated for southern Europe in summer. There, the warming of summers in model simulations of greenhouse-gas-induced climate change is quite strong (Figure A2.1) but interannual variability in 1961-1990 was relatively small, and a relatively large warming of summers was already observed from 1961-1990 to 1991-2008. The recently observed warming and small interannual variability also make the probability of warm summer months (particularly August) large in Iceland, despite a relatively modest warming in climate model simulations. Elsewhere in northern Europe, the differences in model-simulated warming (larger in winter than in summer) and interannual variability (also larger in winter than in summer) have opposing effects, making the seasonal variability in probability irregular. For parts of Turkey, the analysis suggests lower than 50% probability of warm Decembers and Februarys. This peculiarity is caused by a cooling observed from 1961-1990 to 1991-2008, most likely as a result of natural variability.

The probability that the annual mean temperature in the year 2010 (or in any of its near neighbours) exceeds the mean for 1961-1990 is higher than the corresponding probability in any individidual month, varying typically from 80 to 95% with even higher values in the Mediterranean (last panel of Fig. 3.2). These higher probabilities result from the significantly smaller interannual variability of annual than monthly mean temperatures.

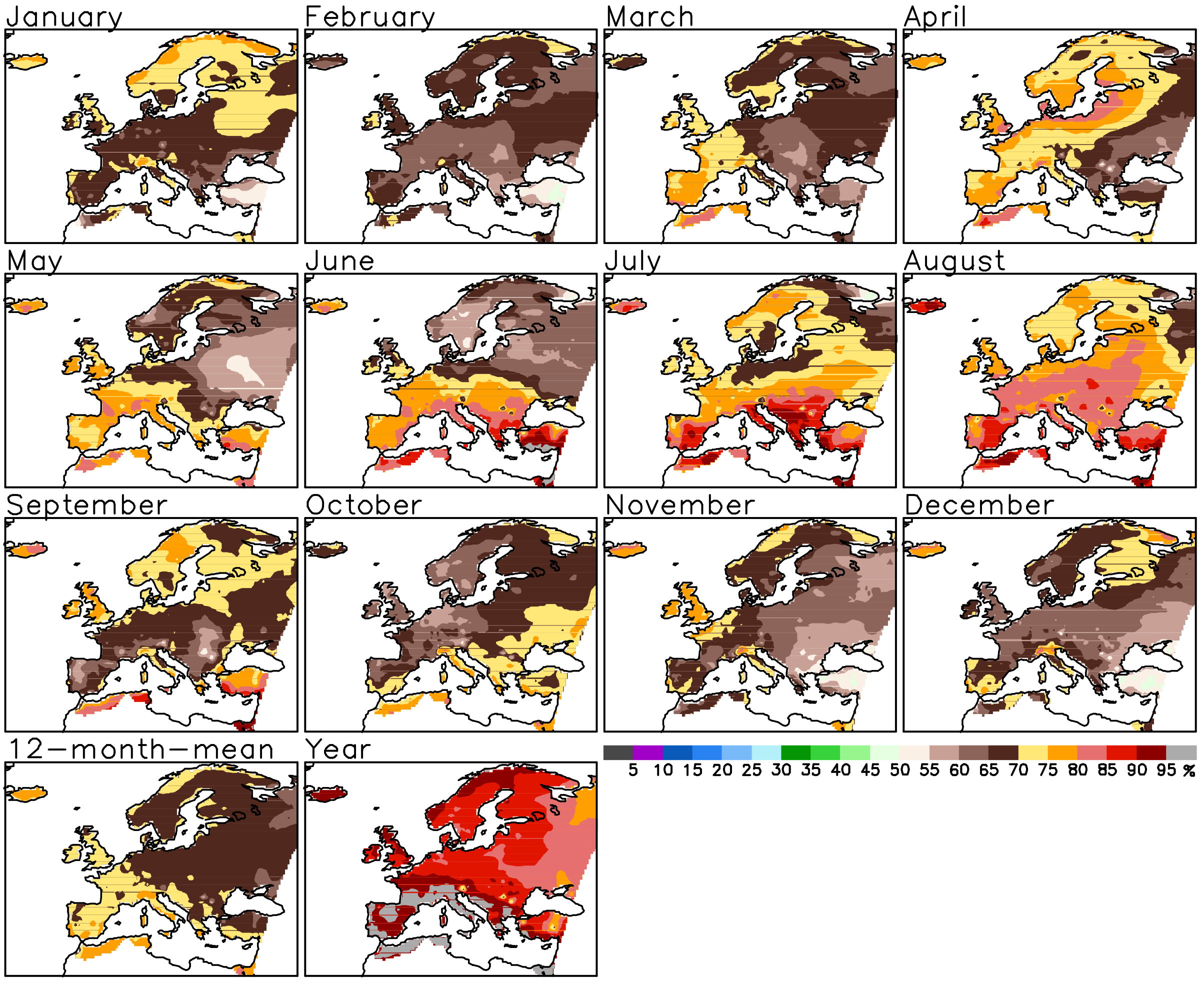

Figure 3.2. *Best-estimate probability of warm months (warmer than the median for 1961-1990) in 2010. The first 12 maps represent the 12 calendar months separately, and the 13th is the average of these 12 maps. The last map shows the corresponding probability of warm years.*

As shown in Fig. 3.3 (first two columns), the probability of warm months and years is projected to increase rapidly with time as the greenhouse-gas-induced climate change proceeds. By the middle of the century, typically about 90% of all months are projected to be warmer than the median for 1961-1990. The probability of warm years is projected to reach this level already by the year 2020, so that, by this time, less than one year per decade would be classified as cold by the 1961-1990 standards.

Corresponding maps for the probability of very warm months and years (above the 90th percentile for 1961-1990) are given in the third and fourth columns of Fig. 3.3. The probability of very warm months, as averaged from January to December, is typically projected to increase from about 20-25% in 2010 to about 50% in 2050. Perhaps surprisingly, a particularly high probability is found in Iceland, most likely as a result of the small interannual variability there. As expected, the probability of very warn years rises even faster than that of warm months – in northern Europe from typically 30-40% in 2010 to about 60-80% in 2030 and to 85-95% or even more in 2050.

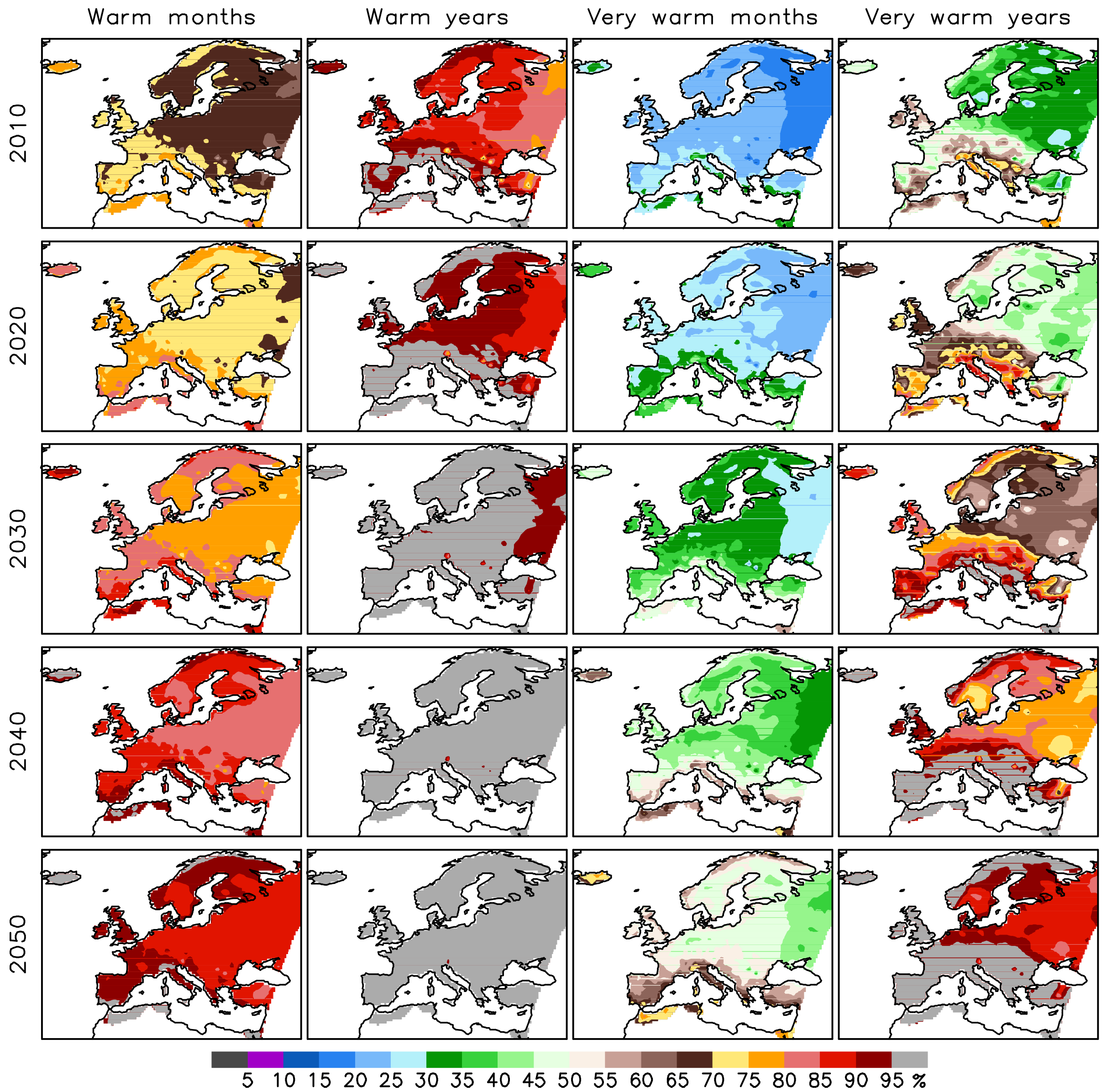

Figure 3.3. *Best-estimate probability of warm and very warm months (mean from December to January) and years as a function of time under the SRES A1B emission scenario. Warm (very warm) months/years are defined as those warmer than the median (90^{th} percentile) observed in 1961-1990.*

A set of more detailed tables, representing the estimated probability distributions of temperature and precipitation variability at individual locations, are provided as an on-line appendix of this report (see Section 5 for more details). As an example, the table for the temperature climate at the station Helsinki Kaisaniemi, Finland, is given as Table 3.1.

Table 3.1. *Probability distributions of monthly (rows 1-6), seasonal (rows 7-8) and annual (row 9) mean temperature in Helsinki, Finland. The first seven columns in each table give the 5th, 10th, 25th, 50th, 75th, 90th and the 95th percentiles of the observed distributions for the periods 1961-1990 (6190) and 1961-2008 (6108) and the model-adjusted distributions for the years 2010, 2030 and 2050. The values are multiplied by 10 (e.g. "-136" means -13.6°C). The last four columns give the probabilities of very cold (VC), cold (C), warm (W) and very warm (VW) months, seasons and years, using threshold temperatures defined by the 10th, 50th and 90th percentiles of the distribution in 1961-1990.*

Helsinki, January

	5%	10%	25%	50%	75%	90%	95%	VC	C	W	VW
6190	-136	-117	-86	-52	-23	-3	8	10	50	50	10
6108	-121	-100	-70	-39	-16	1	11	6	38	62	13
2010	-106	-86	-58	-29	-7	9	18	3	29	71	20
2030	-93	-74	-47	-19	3	18	27	2	21	79	31
2050	-76	-58	-32	-5	16	31	39	1	12	88	48

Helsinki, February

	5%	10%	25%	50%	75%	90%	95%	VC	C	W	VW
6190	-122	-108	-85	-57	-31	-5	9	10	50	50	10
6108	-116	-102	-78	-52	-26	-3	10	7	44	56	11
2010	-102	-90	-68	-42	-17	5	17	3	34	66	16
2030	-90	-78	-56	-31	-7	14	25	1	24	76	23
2050	-73	-62	-41	-17	6	26	37	0	12	88	36

Helsinki, March

	5%	10%	25%	50%	75%	90%	95%	VC	C	W	VW
6190	-65	-56	-39	-20	-3	11	18	10	50	50	10
6108	-61	-51	-34	-15	0	13	20	7	43	57	12
2010	-50	-41	-24	-7	8	20	27	2	30	70	20
2030	-39	-31	-14	2	16	28	34	0	19	81	34
2050	-24	-17	-1	14	27	38	44	0	8	92	56

Helsinki, April

	5%	10%	25%	50%	75%	90%	95%	VC	C	W	VW
6190	10	15	22	30	39	48	54	10	50	50	10
6108	13	17	25	34	45	53	58	7	39	61	18
2010	21	25	32	41	50	57	61	1	20	80	30
2030	29	33	39	48	57	64	68	0	6	94	49
2050	39	42	49	57	66	72	76	0	1	99	76

Helsinki, May

	5%	10%	25%	50%	75%	90%	95%	VC	C	W	VW
6190	74	78	87	97	107	117	122	10	50	50	10
6108	76	80	88	97	107	116	122	8	49	51	8
2010	81	85	93	102	111	121	127	3	35	65	15
2030	87	91	98	107	117	126	132	1	22	78	24
2050	93	98	105	114	124	133	139	0	9	91	41

Helsinki, June

	5%	10%	25%	50%	75%	90%	95%	VC	C	W	VW
6190	123	129	139	150	162	171	175	10	50	50	10
6108	123	128	137	148	161	170	175	11	54	46	8
2010	127	132	141	153	166	175	180	6	45	55	16
2030	132	137	146	158	170	180	184	3	34	66	24
2050	139	143	152	164	177	186	191	1	21	79	36

Helsinki, July

	5%	10%	25%	50%	75%	90%	95%	VC	C	W	VW
6190	148	152	159	168	178	191	200	10	50	50	10
6108	149	154	162	172	184	196	202	8	41	59	16
2010	154	158	166	176	188	200	206	3	29	71	20
2030	159	163	171	181	192	205	211	1	19	81	28
2050	164	169	177	187	199	211	218	0	9	91	40

Helsinki, August

	5%	10%	25%	50%	75%	90%	95%	VC	C	W	VW
6190	138	143	150	157	164	170	173	10	50	50	10
6108	140	144	152	160	169	178	184	9	40	60	23
2010	145	149	157	165	173	182	187	4	25	75	35
2030	150	155	162	170	179	187	192	1	13	87	51
2050	157	161	169	177	185	194	199	0	5	95	72

Helsinki, September

	5%	10%	25%	50%	75%	90%	95%	VC	C	W	VW
6190	86	91	100	110	121	131	136	10	50	50	10
6108	87	93	103	113	124	133	137	8	41	59	12
2010	93	99	108	119	128	137	142	4	28	72	19
2030	99	105	114	124	134	142	147	1	17	83	30
2050	107	113	122	131	140	149	153	0	7	93	50

Helsinki, October

	5%	10%	25%	50%	75%	90%	95%	VC	C	W	VW
6190	36	43	54	64	74	85	92	10	50	50	10
6108	30	39	53	66	78	89	95	13	46	54	15
2010	37	46	60	72	83	93	99	8	33	67	22
2030	44	53	66	78	89	98	104	5	22	78	34
2050	53	62	75	86	96	106	111	2	12	88	54

Helsinki, November

	5%	10%	25%	50%	75%	90%	95%	VC	C	W	VW
6190	-18	-11	1	14	27	39	45	10	50	50	10
6108	-20	-13	0	15	31	43	49	12	49	51	14
2010	-12	-5	8	23	37	48	54	5	35	65	23
2030	-2	5	17	31	45	55	61	1	21	79	35
2050	11	17	28	41	54	64	69	0	8	92	55

Helsinki, December

	5%	10%	25%	50%	75%	90%	95%	VC	C	W	VW
6190	-78	-63	-45	-28	-10	6	17	10	50	50	10
6108	-73	-61	-42	-21	-1	17	26	9	41	59	18
2010	-62	-50	-30	-11	7	23	32	5	28	72	26
2030	-50	-38	-19	-0	17	32	41	2	17	83	40
2050	-33	-22	-4	13	30	44	52	1	7	93	61

Helsinki, Dec-Jan-Feb

	5%	10%	25%	50%	75%	90%	95%	VC	C	W	VW
6190	-95	-87	-69	-46	-26	-12	-4	10	50	50	10
6108	-89	-79	-60	-38	-19	-6	2	6	39	61	16
2010	-76	-67	-49	-28	-11	2	9	1	27	73	26
2030	-64	-55	-38	-18	-1	12	19	0	17	83	41
2050	-48	-40	-23	-4	12	24	31	0	6	94	61

Helsinki, Mar-Apr-May

	5%	10%	25%	50%	75%	90%	95%	VC	C	W	VW
6190	18	21	27	34	44	52	57	10	50	50	10
6108	20	23	30	38	47	55	59	6	40	60	15
2010	28	31	37	44	53	60	64	1	17	83	27
2030	36	39	44	51	60	67	70	0	3	97	47
2050	46	49	54	61	69	76	79	0	0	100	81

Helsinki, Jun-Jul-Aug

	5%	10%	25%	50%	75%	90%	95%	VC	C	W	VW
6190	142	146	152	159	165	171	175	10	50	50	10
6108	143	148	154	161	168	175	179	8	43	57	15
2010	148	152	159	165	172	179	182	3	26	74	27
2030	153	157	163	170	177	184	187	1	13	87	45
2050	159	164	170	177	183	190	194	0	4	96	70

Helsinki, Sep-Oct-Nov

	5%	10%	25%	50%	75%	90%	95%	VC	C	W	VW
6190	44	49	56	63	70	77	82	10	50	50	10
6108	42	48	56	64	73	81	85	12	44	56	16
2010	49	55	63	71	78	85	90	5	24	76	28
2030	56	62	70	77	85	91	96	1	11	89	50
2050	66	72	79	86	93	99	103	0	3	97	79

Helsinki, Annual_Mean

	5%	10%	25%	50%	75%	90%	95%	VC	C	W	VW
6190	36	39	45	52	60	67	70	10	50	50	10
6108	39	42	49	56	63	69	72	6	35	65	15
2010	48	51	57	63	69	74	77	1	11	89	33
2030	55	59	64	70	76	81	84	0	3	97	65
2050	65	69	74	80	85	90	93	0	0	100	93

4. Results for precipitation

In simulations of anthropogenic climate change, changes in precipitation have a much lower signal-to-noise ratio than changes in temperature (e.g., Räisänen and Ruokolainen 2008a; Räisänen and Ruosteenoja 2008). Therefore, the potential to improve estimates of present or near-future precipitation climate by taking climate change into account is rather limited. The main uncertainty in such short-term precipitation projections is natural variability rather than anhtropogenic climate change. In longer-term precipitation projections, however, anthropogenic climate change gradually increases in importance.

The low signal-to-noise ratio of short-term precipitation changes is illustrated in Fig. 4.1. In analogy with Fig. 3.1, probability distributions of monthly precipitation in Helsinki are shown as estimated from observations for 1961-1990 and 1961-2008, and as projected for the year 2010 based on the observations in 1961-2008 and climate model simulations. In some months, there are substantial differences between the distributions derived from data for 1961-1990 and 1961-2008. However, as judged from the small differences between the 2010 and 1961-2008 distributions, these differences are much more likely to reflect natural climate variability than anthropogenic climate change – provided that the magnitude of the latter is not seriously underestimated by climate models. Furthermore, in some months the full period 1961-2008 was drier than its first 30 years 1961-1990, in contrast to the slight increase in precipitation suggested by the models. The most striking example is September. In Helsinki, the median September precipitation of 1961-1990 (71 mm) was exceeded in only four of the 18 Septembers in 1991-2008; thus, the probability of "wet" Septembers in 1961-2008 using the 1961-1990 median as the threshold was only 40%. Even more strikingly, the probability of "very dry" Septembers increased from 10% to 23%. Thus, the division of monthly precipitation totals to different categories is in some cases disturbingly sensitive to the baseline period used for the classification. 1961-2008 would probably be a more representative baseline than 1961-1990 (since it is longer), but for consistency with general practice we use the period 1961-1990 for this purpose.

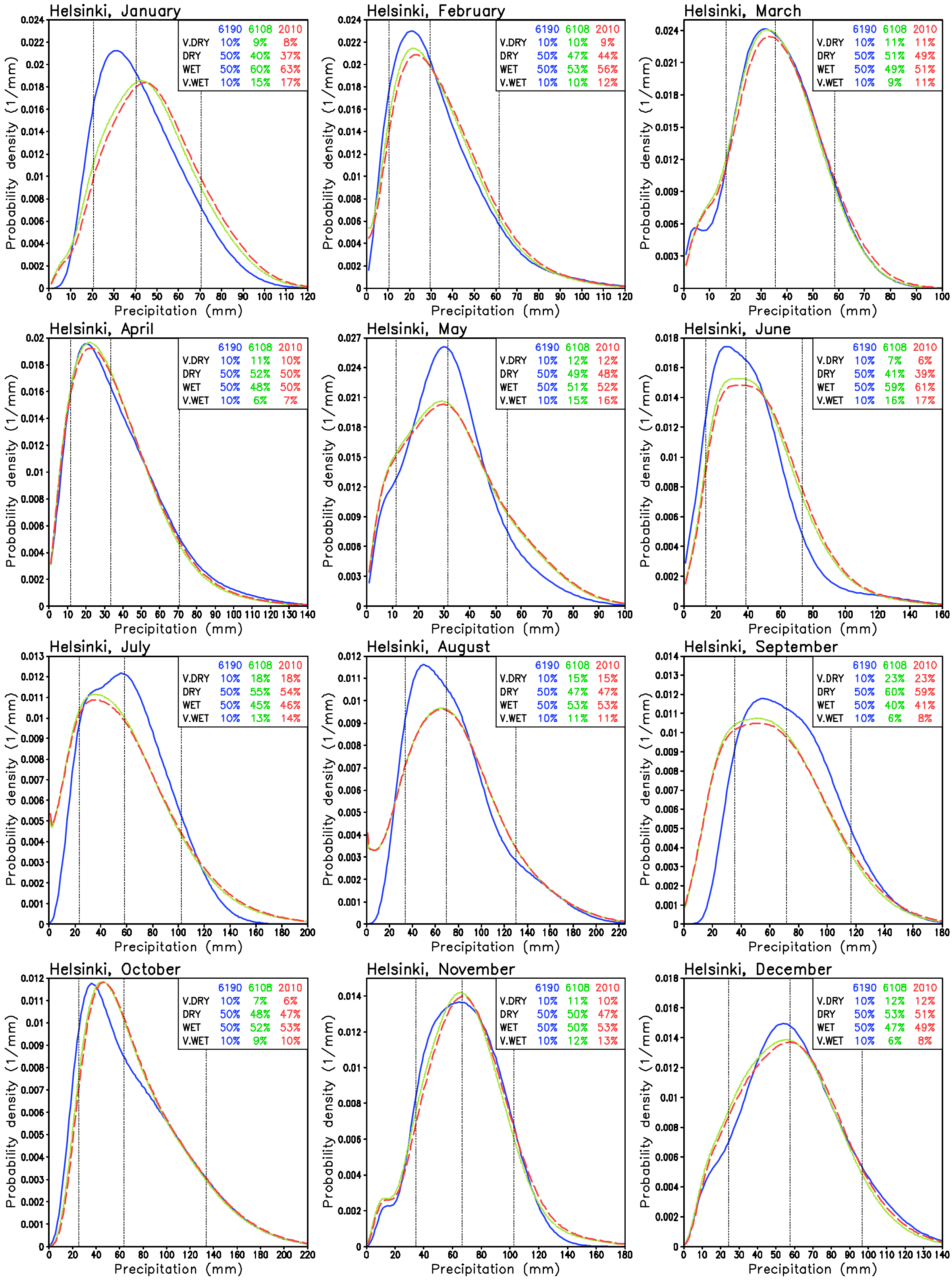

Figure 4.1. *Probability distributions of monthly precipitation in Helsinki, Finland. The blue and the green lines represent the observations for 1961-1990 and 1961-2008, respectively, and the red lines the best-estimate distributions corresponding to the climate in the year 2010. The numbers in the top left corner give the probabilities of very dry, dry, wet and very wet months, using threshold values shown by the three vertical lines. The horizontal and vertical scales vary from month to month.*

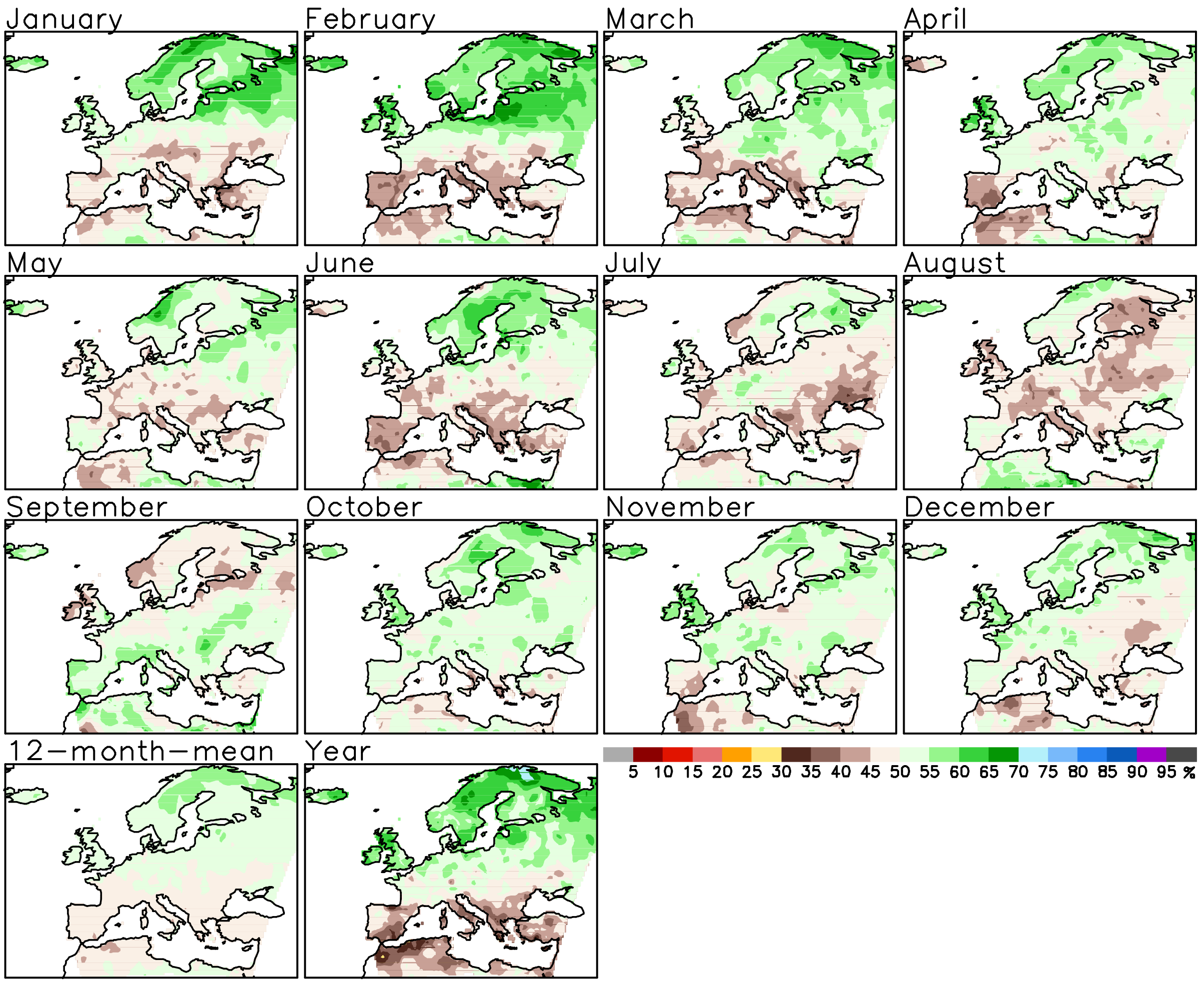

Figure 4.2. *Best-estimate probability of wet months (precipitation above the median for 1961-1990) in 2010. The first 12 maps represent the 12 calendar months separately, and the 13th is the average of these 12 maps. The last map shows the corresponding probability of wet years.*

Similarly to Fig. 3.2, the best-estimate probability of wet months (precipitation above the median of 1961-1990) in the present (year 2010) climate is shown in Fig 4.2. Probabilities exceeding 50% dominate in northern Europe, particularly in winter. Conversely, the probability of wet months in southern Europe is mostly less than 50%. Yet, there is irregularity in these patterns, due to the differences in the observed precipitation climate between the baseline 1961-1990 used for the classification and the period 1961-2002[2] used as the raw material in estimating the climate in 2010. A similar analysis for the year 2050 (Fig. 4.3) reveals a stronger climate change signal, with higher (lower) probabilities in the north (south). At this time, typically about 60% of all months are projected to be wet in northern Europe, although with a substantial variation with the time of the year (generally least wet

[2] In this case, observations were only used up to the year 2002 because of the reason discussed in Appendix A.1. However, in analysing the precipitation climate at individual stations, the full period 1961-2008 was used where available.

months in late summer and most in winter). Considering the annual sum of precipitation (last panel of Fig. 4.3), the probability of wet years around the year 2050 is projected to reach 70-85% in most of Fennoscandia and northwestern Russia. Even so, a comparison between Figs. 4.3 and 3.2 shows that the projected changes in precipitation climate in the middle of this century are still slightly weaker than changes in temperature climate are at present, when putting the changes in the context of interannual variability.

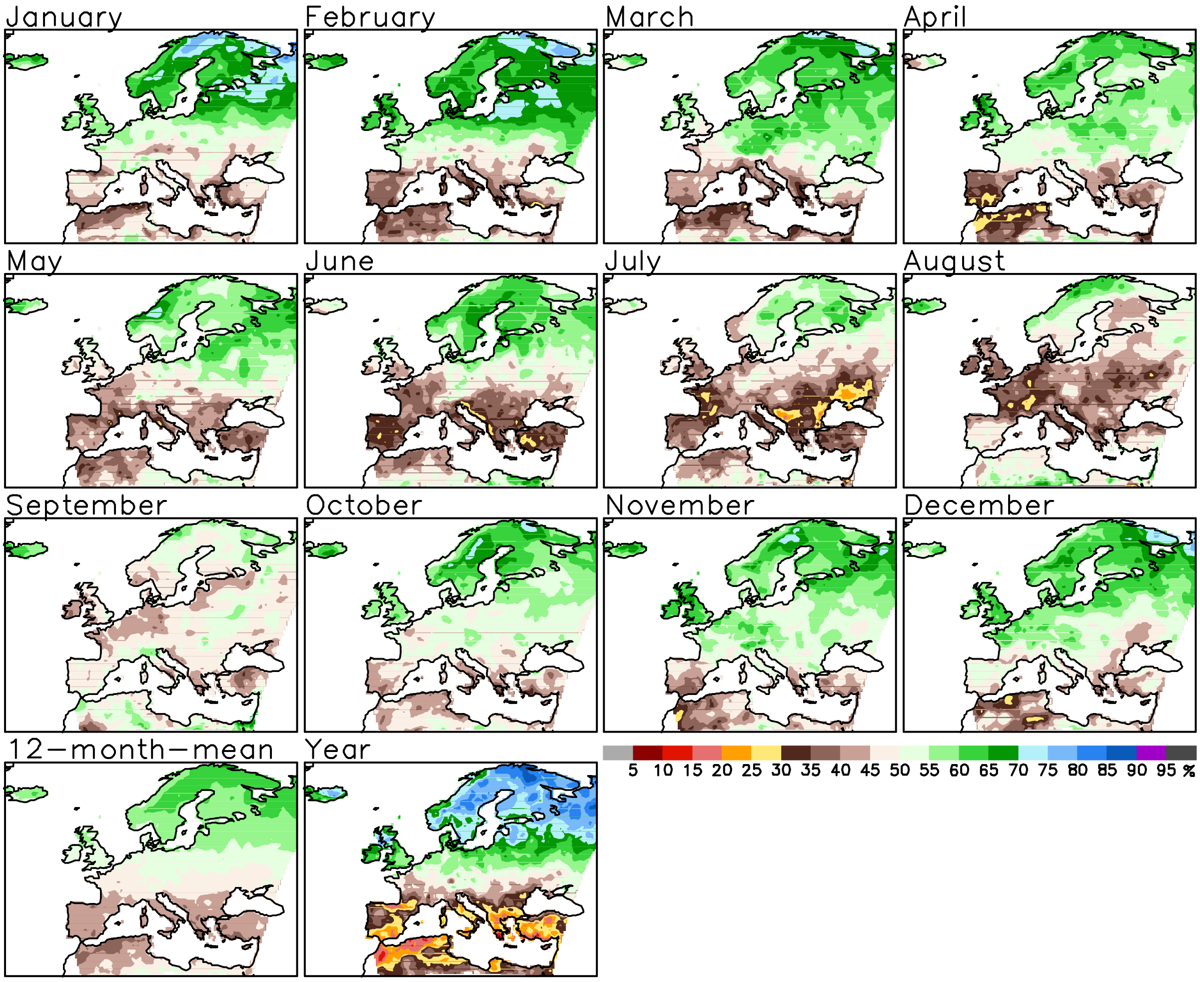

Figure 4.3. *As Figure 4.2, but for the year 2050.*

A more detailed representation of the projected change in precipitation climate at the station Helsinki Kaisaniemi is given in Table 4.1. In addition to a general increase in the probability of wet months at the expense of dry months, the analysis also suggests a gradual increase in the probability of very wet (above the 90th percentile in 1961-1990) months with time. Changes in the dry end of the precipitation distribution are less systematic. As judged from the 5th percentile (leftmost column in each panel), the driest winter months are projected to become less dry but a slight signal towards to the opposite direction is seen in some of the summer months, despite a small increase in median (and mean) precipitation. In some months, the changes projected between 2010 and 2050 are small compared with the

Table 4.1. *Probability distributions of monthly (rows 1-6), seasonal (rows 7-8) and annual (row 9) precipitation in Helsinki, Finland. The first seven columns in each table give the 5th, 10th, 25th, 50th, 75th, 90th and the 95th percentiles of the observed distributions for the periods 1961-1990 (6190) and 1961-2008 (6108) and the model-adjusted distributions for the years 2010, 2030 and 2050 (unit: mm). The last four columns give the probabilities of very dry (VD), dry (D), wet (W) and very wet (VW) months, seasons and years, using threshold values defined by the 10th, 50th and 90th percentiles of the distribution in 1961-1990.*

Helsinki, January

	5%	10%	25%	50%	75%	90%	95%	VD	D	W	VW
6190	16	20	28	40	55	70	79	10	50	50	10
6108	16	21	31	45	61	76	85	9	40	60	15
2010	17	22	33	47	63	78	87	8	37	63	17
2030	18	24	35	49	66	81	91	7	33	67	20
2050	20	25	37	52	69	85	95	5	30	70	23

Helsinki, February

	5%	10%	25%	50%	75%	90%	95%	VD	D	W	VW
6190	8	11	18	29	44	61	74	10	50	50	10
6108	7	11	19	31	46	62	73	10	47	53	10
2010	8	12	20	32	48	64	75	9	44	56	12
2030	8	12	21	33	49	66	77	8	42	58	13
2050	9	13	22	35	51	69	80	7	39	61	15

Helsinki, March

	5%	10%	25%	50%	75%	90%	95%	VD	D	W	VW
6190	10	16	25	36	47	58	64	10	50	50	10
6108	10	15	24	35	47	58	64	11	51	49	9
2010	10	15	25	36	48	59	66	11	49	51	11
2030	10	16	26	37	50	61	68	11	46	54	13
2050	10	16	27	39	52	64	71	10	44	56	16

Helsinki, April

	5%	10%	25%	50%	75%	90%	95%	VD	D	W	VW
6190	8	11	19	33	52	71	85	10	50	50	10
6108	7	11	19	32	49	67	79	11	52	48	6
2010	7	11	19	33	50	68	81	10	50	50	7
2030	7	11	20	33	51	70	83	10	49	51	9
2050	7	11	20	34	53	72	85	10	48	52	11

Helsinki, May

	5%	10%	25%	50%	75%	90%	95%	VD	D	W	VW
6190	7	12	21	31	42	55	64	10	50	50	10
6108	7	10	19	32	46	62	71	12	49	51	15
2010	7	10	19	32	47	62	72	12	48	52	16
2030	7	10	20	33	48	63	73	12	47	53	17
2050	7	11	20	33	49	65	74	11	45	55	18

Helsinki, June

	5%	10%	25%	50%	75%	90%	95%	VD	D	W	VW
6190	9	14	24	38	55	73	90	10	50	50	10
6108	12	17	27	44	63	83	96	7	41	59	16
2010	12	17	28	45	65	84	98	6	39	61	17
2030	13	18	29	47	67	87	101	6	38	62	19
2050	13	19	30	49	69	91	106	6	36	64	22

Helsinki, July

	5%	10%	25%	50%	75%	90%	95%	VD	D	W	VW
6190	18	24	37	59	82	103	115	10	50	50	10
6108	9	16	30	53	81	111	130	18	55	45	13
2010	9	16	31	54	83	113	133	18	54	46	14
2030	8	15	31	55	85	115	136	18	54	46	15
2050	8	15	31	56	87	119	140	17	52	48	16

Helsinki, August

	5%	10%	25%	50%	75%	90%	95%	VD	D	W	VW
6190	27	33	47	69	97	131	152	10	50	50	10
6108	14	25	46	72	102	135	156	15	47	53	11
2010	14	25	46	72	103	135	156	15	47	53	11
2030	14	25	46	72	103	135	157	15	47	53	11
2050	13	25	46	73	103	136	158	15	47	53	12

Helsinki, September

	5%	10%	25%	50%	75%	90%	95%	VD	D	W	VW
6190	30	36	50	71	95	117	130	10	50	50	10
6108	16	22	38	61	87	112	127	23	60	40	6
2010	16	22	38	62	89	114	130	23	59	41	8
2030	15	22	38	63	91	116	132	22	58	42	10
2050	15	22	39	64	93	119	136	22	57	43	11

Helsinki, October

	5%	10%	25%	50%	75%	90%	95%	VD	D	W	VW
6190	19	25	39	63	99	133	154	10	50	50	10
6108	23	29	43	65	98	132	153	7	48	52	9
2010	24	30	44	67	99	134	155	6	47	53	10
2030	25	31	45	68	101	136	157	5	45	55	11
2050	26	33	47	70	103	139	160	4	43	57	12

Helsinki, November

	5%	10%	25%	50%	75%	90%	95%	VD	D	W	VW
6190	26	34	48	67	86	102	111	10	50	50	10
6108	23	33	48	67	86	105	118	11	50	50	12
2010	24	34	50	69	89	108	121	10	47	53	13
2030	25	35	52	71	91	111	124	9	44	56	15
2050	27	37	54	74	95	114	128	8	40	60	18

Helsinki, December

	5%	10%	25%	50%	75%	90%	95%	VD	D	W	VW
6190	17	25	40	58	77	97	108	10	50	50	10
6108	15	22	36	55	75	93	104	12	53	47	6
2010	16	23	38	57	77	95	106	12	51	49	8
2030	17	24	39	59	79	97	109	11	49	51	10
2050	18	25	41	61	81	100	112	10	46	54	12

Helsinki, Dec–Jan–Feb

	5%	10%	25%	50%	75%	90%	95%	VD	D	W	VW
6190	73	83	103	135	166	191	209	10	50	50	10
6108	67	80	105	138	168	195	213	11	48	52	12
2010	70	83	110	142	174	201	218	10	44	56	14
2030	73	87	114	148	180	208	225	8	40	60	18
2050	77	92	120	154	188	216	235	7	35	65	22

Helsinki, Mar–Apr–May

	5%	10%	25%	50%	75%	90%	95%	VD	D	W	VW
6190	55	64	83	106	129	150	162	10	50	50	10
6108	56	65	83	105	127	148	161	10	51	49	9
2010	57	66	84	107	130	152	165	9	49	51	11
2030	58	67	86	110	133	155	169	8	46	54	13
2050	60	69	88	113	137	160	174	7	43	57	16

Helsinki, Jun–Jul–Aug

	5%	10%	25%	50%	75%	90%	95%	VD	D	W	VW
6190	90	106	136	174	215	262	291	10	50	50	10
6108	80	99	134	177	226	281	312	12	48	52	14
2010	80	100	136	180	230	286	318	12	47	53	15
2030	81	101	138	183	234	292	325	11	45	55	17
2050	81	103	140	187	241	300	335	11	43	57	18

Helsinki, Sep–Oct–Nov

	5%	10%	25%	50%	75%	90%	95%	VD	D	W	VW
6190	118	135	167	210	253	291	321	10	50	50	10
6108	108	128	163	205	246	283	308	12	53	47	6
2010	112	131	167	209	251	288	314	11	50	50	8
2030	115	135	172	214	256	294	319	10	47	53	11
2050	120	140	177	220	263	301	326	8	44	56	13

Helsinki, Annual_Sum

	5%	10%	25%	50%	75%	90%	95%	VD	D	W	VW
6190	462	494	556	629	708	784	831	10	50	50	10
6108	453	491	558	632	708	779	823	11	49	51	9
2010	466	504	572	646	722	794	839	8	44	56	12
2030	478	517	586	661	739	813	858	7	39	61	15
2050	494	535	605	682	761	836	883	5	32	68	20

differences between the two baseline periods 1961-1990 and 1961-2008, implying that the uncertainty in the baseline precipitation climate may be a larger issue than the greenhouse-gas-induced change during the first half of this century. This holds, in particular, for the tails of the distributions (the dry end of the September distribution might be regarded as a nightmare example!). However, when considering precipitation on seasonal and annual time scales, the baseline sampling uncertainty becomes relatively less important in comparison with climate change.

5. Tables for individual locations

Tables 3.1 and 4.1 above provided estimates of the probability distributions of temperature and precipitation variability for Helsinki, Finland. Similar tables were produced for a total of 120 locations for temperature and for 230 locations for precipitation (Figure 5.1). The calculation combined observations collected within the European Climate Assessment & Dataset (ECA&D) project (Klein Tank et al. 2002; http://eca.knmi.nl/) with the global CMIP3 and regional ENSEMBLES model simulations. The selected set of stations includes nearly all Nordic (Finland, Sweden, Norway, Denmark and Iceland) stations in the ECA&D database, for which data were available for at least 44 out of the 48 years in 1961-2008. In the case of precipitation, a few stations were rejected because of strongly suspected quality problems (e.g., spuriously many months with zero precipitation). The resulting set of temperature stations is reasonably well distributed across the Nordic countries; for precipitation, however, the station density is high in Norway but much lower in the other four countries.

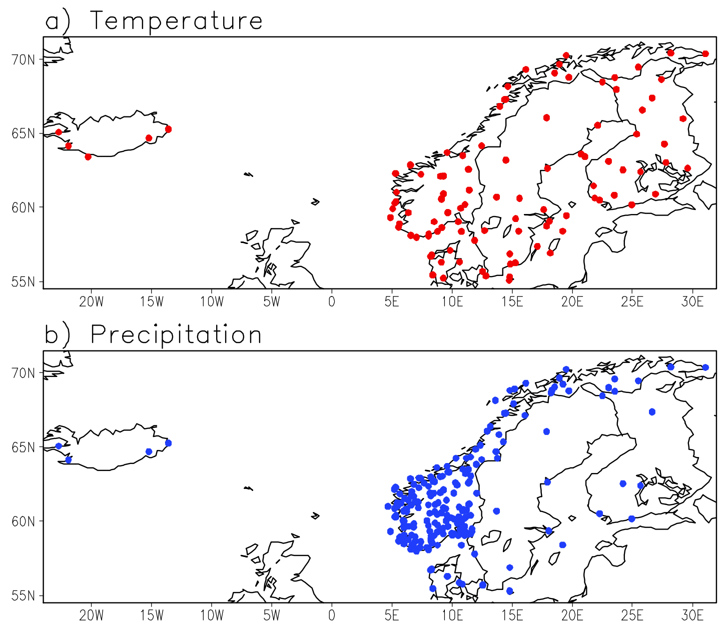

Figure 5.1. *Locations of the stations for which tables similar to Table 3.1 and Table 4.1 are available at http://www.atm.helsinki.fi/~jaraisan/CES_D2.4/Tables_T and http://www.atm.helsinki.fi/~jaraisan/CES_D2.4/Tables_P. (a) temperature, (b) precipitation.*

The stations used in the analysis are listed in Table 5.1. The actual temperature and precipitation tables are available in pdf format at http://www.atm.helsinki.fi/~jaraisan/CES_D2.4/Tables_T and http://www.atm. helsinki.fi/~jaraisan/CES_D2.4/Tables_P.

In constructing these tables, it was assumed that the signal of anthropogenic climate change varies smoohtly in space and can therefore be estimated from global and regional climate model simulations. To the extent that this assumption is violated, for example due to local water bodies and small-scale variations in torography, such variations are not captured by the present method. Thus, differences between the probability distributions calculated for nearby locations originate directly from the differences in the local observed climate.

Table 5.1. *List of the stations for which tables similar to Table 3.1 and Table 4.1 have been prepared.*

```
--------------------------------------------------------------------------
STAID = ECA&D STATION IDENTIFIER     NAME =STATION NAME
CN = COUNTRY CODE                    HGT = HEIGHT ABOVE SEA LEVEL
T = TABLES AVAILABLE FOR TEMPERATURE P = TABLES AVAILABLE FOR PRECIPITATION
--------------------------------------------------------------------------
```

STAID	NAME	CN	LATITUDE	LONGITUDE	HGT	
1	VAEXJOE	SE	+56:52:00	+14:48:00	166	TP
2	FALUN	SE	+60:37:00	+15:37:00	160	T
4	LINKOEPING	SE	+58:24:00	+15:31:59	93	T
5	LINKOEPING-MALMSLAETT	SE	+58:24:00	+15:31:59	93	T
8	OESTERSUND	SE	+63:10:59	+14:28:59	376	T
9	OESTERSUND-FROESOEN	SE	+63:10:59	+14:28:59	376	T
10	STOCKHOLM	SE	+59:21:00	+18:03:00	44	P
28	HELSINKI	FI	+60:10:00	+24:57:00	4	TP
29	JYVASKYLA	FI	+62:24:00	+25:40:59	137	TP
30	SODANKYLA	FI	+67:22:00	+26:39:00	179	TP
65	DALATANGI	IS	+65:16:00	-13:34:59	9	TP
66	REYKJAVIK	IS	+64:07:59	-21:54:00	52	TP
67	STYKKISHOLMUR	IS	+65:04:24	-22:43:39	14	TP
68	TEIGARHORN	IS	+64:40:59	-15:13:39	22	TP
69	VESTMANNAEYJAR	IS	+63:24:00	-20:16:59	118	T
106	HAMMER ODDE FYR	DK	+55:18:00	+14:46:59	11	TP
107	VESTERVIG	DK	+56:46:00	+08:19:00	18	TP
108	GRONBAEK-ALLINGSKOVGARD	DK	+56:16:59	+09:37:00	25	P
109	NORDBY (FANO)	DK	+55:27:00	+08:24:00	4	TP
113	TRANEBJERG	DK	+55:51:00	+10:36:00	11	P
114	KOEBENHAVN - METEOROLOGISK INS	DK	+55:43:00	+12:34:00	8	P
115	KOEBENHAVN: BOTANISK HAVE	DK	+55:40:59	+12:34:59	6	P
116	KOEBENHAVN: LANDBOHOJSKOLEN-1	DK	+55:40:59	+12:31:59	9	TP
117	HAMMER ODDE FYR-1	DK	+55:18:00	+14:46:59	11	TP
118	SANDVIG	DK	+55:16:59	+14:46:59	12	TP
119	KOEBENHAVN: LANDBOHOJSKOLEN	DK	+55:40:59	+12:31:59	9	T
178	BARKESTAD	NO	+68:49:00	+14:48:00	3	P
180	LIEN I SELBU	NO	+63:12:32	+11:06:56	255	P
181	MESTAD I ODDERNES	NO	+58:12:55	+07:53:26	151	P
183	NORD ODAL	NO	+60:23:18	+11:33:37	147	P
184	HALDEN	NO	+59:07:21	+11:23:18	8	P
185	SUOLOVUOPMI	NO	+69:35:17	+23:31:54	377	P
188	GLOMFJORD	NO	+66:49:00	+13:58:59	39	T
190	KARASJOK	NO	+69:28:00	+25:30:11	129	TP
191	KJOEREMSGRENDE	NO	+62:06:00	+09:03:00	626	T

192	FAERDER FYR	NO	+59:01:36	+10:31:48	6	TP
193	OSLO BLINDERN	NO	+59:56:34	+10:43:14	94	TP
194	UTSIRA FYR	NO	+59:18:28	+04:52:41	55	TP
195	VARDOE	NO	+70:22:01	+31:05:04	14	TP
196	NESBYEN-SKOGLUND	NO	+60:34:06	+09:07:18	167	TP
197	BULKEN	NO	+60:38:45	+06:13:24	323	P
264	OKSOEY FYR	NO	+58:04:00	+08:03:02	9	TP
265	BERGEN FLORIDA	NO	+60:22:59	+05:19:59	12	TP
266	BODOE VI	NO	+67:16:01	+14:21:32	11	TP
302	TRANEBJERG OST	DK	+55:51:00	+10:36:00	11	P
303	VESTERVIG-1	DK	+56:46:00	+08:19:00	18	T
304	NORDBY (FANO)-1	DK	+55:27:00	+08:24:00	4	T
328	TROMSO	NO	+69:39:14	+18:55:41	100	TP
329	ONA II	NO	+62:51:34	+06:32:21	13	TP
330	FOKSTUA	NO	+62:07:00	+09:16:59	952	TP
331	TORUNGEN FYR	NO	+58:22:59	+08:47:30	12	TP
340	HOLMOGADD	SE	+63:36:00	+20:45:00	5	T
341	MALUNG	SE	+60:40:59	+13:42:00	308	TP
342	GOTSKA SANDON	SE	+58:24:00	+19:12:00	11	TP
426	UPPSALA	SE	+59:51:36	+17:37:48	13	T
462	GOTEBORG	SE	+57:46:59	+11:52:59	20	TP
466	HARNOSAND	SE	+62:37:59	+17:55:59	15	TP
671	FSN ALBORG	DK	+57:06:00	+09:51:00	3	T
672	FSN KARUP	DK	+56:18:00	+09:07:12	52	T
673	TIRSTRUP	DK	+56:19:12	+10:37:48	25	T
674	FSN SKRYDSTRUP	DK	+55:13:48	+09:16:12	41	T
676	ROSNAES FYR	DK	+55:45:00	+10:52:12	14	P
677	BORNHOLMS LUFTHAVN	DK	+55:04:12	+14:45:00	15	T
704	PORI AIRPORT	FI	+61:27:00	+21:46:48	10	T
705	MIETOINEN SAARI	FI	+60:37:48	+21:52:12	13	T
706	TURKU AIRPORT	FI	+60:30:00	+22:16:12	47	TP
708	JOKIOINEN OBSERVATOR	FI	+60:49:12	+23:30:00	104	T
710	UTTI AIRPORT/VALKEAL	FI	+60:54:00	+26:55:48	99	T
717	KAUHAVA AIRPORT	FI	+63:06:00	+23:01:48	42	T
718	AHTARI MYLLYMAKI	FI	+62:31:48	+24:13:12	157	TP
721	KUOPIO AIRPORT/SIILI	FI	+63:01:12	+27:48:00	94	T
723	JOENSUU AIRPORT/LIPE	FI	+62:39:00	+29:36:00	118	T
725	KAJAANI AIRPORT	FI	+64:16:12	+27:40:12	134	T
727	OULU AIRPORT/OULUNSA	FI	+64:55:48	+25:22:12	12	T
732	KUUSAMO AIRPORT	FI	+65:58:48	+29:13:12	264	T
733	ROVANIEMI AIRPORT/RO	FI	+66:34:11	+25:49:48	195	T
734	MUONIO KK ALAMUONIO	FI	+67:58:12	+23:40:12	254	T
735	INARI/IVALO AIRPORT	FI	+68:36:59	+27:25:12	144	T
942	KARASJOK-MARKANNJARGA	NO	+69:27:48	+25:30:07	131	TP
953	NESBYEN-TODOKK	NO	+60:34:01	+09:08:00	166	TP
955	SUOLOVUOPMI-LULIT	NO	+69:34:46	+23:32:03	381	P
1040	ROROS	NO	+62:34:01	+11:23:00	628	TP
1041	KONGSBERG IV	NO	+59:39:47	+09:39:00	168	TP
1042	LYNGOR FYR	NO	+58:38:00	+09:09:01	4	T
1043	TVEITSUND	NO	+59:01:37	+08:31:14	252	TP
1044	LINDESNES FYR	NO	+57:58:59	+07:02:53	13	TP
1045	LISTA FYR	NO	+58:06:36	+06:34:05	14	TP
1046	SOLA	NO	+58:53:03	+05:38:12	7	TP
1047	SAUDA	NO	+59:38:54	+06:21:47	5	TP
1048	GARDERMOEN	NO	+60:12:23	+11:04:49	202	TP
1049	TAKLE	NO	+61:01:36	+05:23:06	38	TP
1050	SVINOY	NO	+62:17:24	+05:18:00	38	TP
1051	TAFJORD	NO	+62:14:00	+07:25:00	15	T
1052	VAERNES	NO	+63:30:00	+10:53:24	12	TP
1053	RENA - HAUGEDALEN	NO	+61:09:33	+11:26:33	240	TP
1054	KJOBLI I SNAASA	NO	+64:09:36	+12:28:12	195	TP
1055	ORLAND	NO	+63:42:01	+09:36:05	10	TP
1056	SKROVA FYR	NO	+68:09:01	+14:39:02	11	T
1057	BARDUFOSS	NO	+69:03:32	+18:32:25	76	TP
1058	SIHCCAJAVRI	NO	+68:45:19	+23:32:18	382	TP
1059	FRUHOLMEN FYR	NO	+71:05:35	+23:59:42	13	T
1060	RUSTEFJELBMA	NO	+70:24:01	+28:12:01	10	TP
1409	KARESUANDO	SE	+68:27:00	+22:30:00	327	TP

1412	LULEA FLYGPLATS	SE	+65:32:24	+22:07:12	17	T
1413	HARSFJARDEN	SE	+59:04:12	+18:07:12	4	T
1414	SVENSKA HOGARNA	SE	+59:26:24	+19:30:36	12	T
1415	SAVE	SE	+57:46:48	+11:52:48	20	TP
1416	SATENAS	SE	+58:26:24	+12:42:36	54	T
1418	FALSTERBO	SE	+55:22:48	+12:49:12	5	T
1419	BREDAKRA	SE	+56:15:36	+15:16:12	58	T
1420	HOBURG	SE	+56:55:12	+18:09:59	38	T
1421	KARLSHAMN	SE	+56:10:48	+14:51:00	50	T
1423	OLANDS NORRA UDDE	SE	+57:22:12	+17:06:00	4	T
1424	LANDSORT	SE	+58:44:24	+17:52:12	18	T
1425	OREBRO	SE	+59:14:24	+15:17:24	35	T
1428	ARJEPLOG	SE	+66:03:00	+17:52:12	431	TP
2162	THYBORON-1	DK	+56:42:00	+08:13:12	3	TP
2215	ANDOYA	NO	+69:18:00	+16:08:59	14	TP
2230	BERGEN/FLESLAND	NO	+60:17:21	+05:13:35	48	TP
2272	VALASSAARET	FI	+63:25:48	+21:04:12	4	T
2574	FOKSTUGU	NO	+62:06:51	+09:17:13	972	TP
2575	KONGSBERG II/III	NO	+59:39:47	+09:38:53	171	TP
2576	KONGSBERG BRANNSTASJON	NO	+59:37:28	+09:38:16	170	TP
2577	NESBYEN	NO	+60:34:00	+09:06:00	164	TP
2578	NESBYEN II	NO	+60:34:00	+09:07:59	165	TP
2579	ROROS AIRPORT	NO	+62:34:37	+11:21:06	625	TP
2580	RENA	NO	+61:07:59	+11:22:59	225	P
2581	ONA	NO	+62:52:00	+06:33:00	11	TP
2582	ONA HUSOY	NO	+62:52:00	+06:31:59	8	TP
2583	HVALER	NO	+59:02:09	+11:03:06	17	P
2584	BREKKE SLUSE	NO	+59:08:52	+11:33:34	114	P
2586	IGSI I HOBOL	NO	+59:38:08	+11:02:52	144	P
2587	RADE - TOMB	NO	+59:19:00	+10:49:00	14	P
2588	ORJE	NO	+59:28:51	+11:39:06	123	P
2589	RYGGE	NO	+58:22:59	+10:47:17	40	TP
2590	SARPSBORG	NO	+59:17:08	+11:06:52	57	P
2591	STROMSFOSS SLUSE	NO	+59:18:02	+11:39:38	113	P
2592	MOSS	NO	+59:26:02	+10:40:00	31	P
2593	MOSS BRANNSTASJON	NO	+59:26:34	+10:41:03	32	P
2594	ASKER	NO	+59:51:21	+10:26:12	163	P
2595	EIDSVOLL VERK	NO	+60:17:53	+11:09:47	181	P
2596	BJORNHOLT	NO	+60:03:03	+10:41:11	360	P
2597	KJELSAS I SORKEDALEN	NO	+60:02:13	+10:35:52	319	P
2598	MARIDALSOSET	NO	+59:58:08	+10:47:35	173	P
2599	NORDSTRAND	NO	+59:52:22	+10:47:33	118	P
2601	ATNSJOEN	NO	+61:53:25	+10:08:30	749	P
2602	BLANKTJERNMOEN I KVIKNE	NO	+62:25:58	+10:25:01	690	P
2603	DREVSJO	NO	+61:53:13	+12:02:53	672	P
2604	JONSBERG LANDBRUKSSKOLE	NO	+60:45:03	+11:12:23	218	P
2606	KVIKNE I OSTERDAL	NO	+62:35:48	+10:16:17	550	P
2607	NES PA HEDMARK	NO	+60:47:29	+10:57:32	205	P
2609	BEITO	NO	+61:14:35	+08:51:20	754	P
2610	BIRI	NO	+60:57:10	+10:35:49	190	P
2611	ABJORSBRATEN	NO	+60:55:05	+09:17:25	639	TP
2612	BOVERDAL	NO	+61:43:14	+08:14:39	701	P
2613	ESPEDALEN	NO	+61:25:00	+09:32:04	752	P
2614	LUNNER	NO	+60:17:39	+10:34:49	372	P
2616	PRESTSTULEN	NO	+61:55:17	+09:00:47	823	P
2617	REINLI	NO	+60:50:07	+09:29:35	628	P
2618	SKJAK	NO	+61:54:06	+08:10:19	432	P
2619	SKJAK II	NO	+61:52:40	+08:28:18	372	P
2620	OSTRE TOTEN - APELSVOLL	NO	+60:42:00	+10:52:00	264	P
2621	VANG I VALDRES	NO	+61:07:33	+08:34:54	477	P
2623	ASK PA RINGERIKE	NO	+60:08:21	+10:10:36	77	P
2625	GEILO	NO	+60:31:54	+08:08:53	841	P
2626	GRIMELI I KRODSHERAD	NO	+60:08:16	+09:35:48	367	P
2627	GULSVIK II	NO	+60:22:58	+09:36:24	142	P
2628	HIASEN I SIGDAL	NO	+60:00:43	+09:30:36	402	P
2629	HOLE	NO	+60:06:32	+10:17:48	66	P
2630	AL III	NO	+60:38:18	+08:33:57	706	P
2631	SOKNA II	NO	+60:14:17	+09:55:33	140	P

2632	TUNHOVD	NO	+60:27:48	+08:45:09	870	P
2633	HEDRUM	NO	+59:11:44	+09:58:05	31	P
2634	LARVIK	NO	+59:03:11	+10:01:37	28	P
2635	SANDEFJORD	NO	+59:07:58	+10:12:59	6	P
2637	FOLDSAE	NO	+59:19:26	+08:09:07	532	P
2638	GVARV	NO	+59:22:59	+09:10:59	26	P
2639	GVARV - LINDEM	NO	+59:23:12	+09:12:06	71	P
2641	HOIDALEN I SOLUM	NO	+59:08:39	+09:16:01	113	P
2642	KILEGREND	NO	+59:00:33	+08:16:24	287	P
2643	LIFJELL	NO	+59:27:18	+09:02:13	354	P
2644	MOGEN	NO	+60:01:05	+07:54:52	954	P
2645	NOTODDEN	NO	+59:33:00	+09:15:51	34	P
2646	POSTMYR I DRANGEDAL	NO	+59:15:52	+08:46:30	464	P
2647	RAULAND	NO	+59:42:16	+08:02:11	715	P
2648	RJUKAN	NO	+59:52:45	+08:34:35	300	P
2649	TUDDAL	NO	+59:44:43	+08:48:36	464	P
2651	HEREFOSS	NO	+58:31:01	+08:21:12	85	P
2652	MYKLAND	NO	+58:37:59	+08:16:54	245	P
2653	TOVDAL	NO	+58:47:35	+08:14:03	227	P
2654	BAKKE	NO	+58:24:42	+06:39:29	75	P
2655	FEDAFJORDEN II	NO	+58:16:54	+06:49:05	26	P
2656	KJEVIK	NO	+58:12:01	+08:04:05	12	TP
2657	RISNES I FJOTLAND	NO	+58:39:28	+06:56:47	348	P
2658	ASERAL	NO	+58:36:56	+07:24:24	278	P
2659	VIGMOSTAD	NO	+58:13:19	+07:20:13	38	P
2660	OVRE SIRDAL	NO	+58:56:47	+06:55:09	582	P
2661	FLEKKEFJORD	NO	+58:17:03	+06:38:58	5	P
2662	BJORHEIM I RYFYLKE	NO	+59:04:39	+06:01:12	64	P
2663	EGERSUND	NO	+58:27:10	+06:00:11	4	P
2664	HOGNESTAD	NO	+58:41:40	+05:38:30	19	P
2665	HUNDSEID I VIKEDAL	NO	+59:33:20	+05:59:44	159	P
2667	LYSEBOTN	NO	+59:03:24	+06:38:57	9	P
2668	MAUDAL	NO	+58:45:57	+06:22:10	311	P
2669	OBRESTAD FYR	NO	+58:39:33	+05:33:19	24	TP
2670	SOYLAND I GJESDAL	NO	+58:41:03	+05:59:04	263	P
2671	STAVANGER - VALAND	NO	+58:57:25	+05:43:48	72	P
2672	SULDALSVATN	NO	+59:35:18	+06:48:32	333	P
2673	SVILAND	NO	+58:49:06	+05:55:13	230	P
2674	EKSINGEDAL	NO	+60:48:10	+06:09:01	450	P
2675	ETNE	NO	+59:39:52	+05:57:56	35	P
2676	FANA - STEND	NO	+60:16:23	+05:19:53	54	P
2678	FROYSET	NO	+60:50:53	+05:13:01	13	P
2679	GULLBRA	NO	+60:49:44	+06:15:00	579	P
2680	HATLESTRAND	NO	+60:02:31	+05:54:20	45	P
2682	OVSTEDAL	NO	+60:41:18	+05:57:52	316	P
2683	ROLDAL	NO	+59:49:45	+06:49:31	393	P
2684	ROSENDAL	NO	+59:59:27	+06:01:26	51	P
2685	SLATTEROY FYR	NO	+59:54:29	+05:04:05	25	T
2686	ALFOTEN II	NO	+61:49:54	+05:40:06	24	P
2687	AURLAND	NO	+60:54:11	+07:12:06	15	P
2688	BOTNEN I FORDE	NO	+61:32:09	+06:03:37	237	P
2689	BREKKE I SOGN	NO	+60:57:33	+05:25:36	240	P
2690	BRIKSDAL	NO	+61:41:39	+06:48:34	40	P
2691	HAFSLO	NO	+61:17:33	+07:11:18	246	P
2692	HAUKEDAL	NO	+61:25:13	+06:22:32	329	P
2693	HORNINDAL	NO	+62:00:11	+06:39:03	340	P
2694	HOVLANDSDAL	NO	+61:14:03	+05:25:55	60	P
2695	LAVIK	NO	+61:06:43	+05:32:48	31	P
2696	MARISTOVA	NO	+61:06:33	+08:02:09	806	P
2697	MYKLEBUST I BREIM	NO	+61:42:48	+06:36:59	315	P
2698	RORVIKVATN VED VADHEIM	NO	+61:12:59	+05:45:05	350	P
2699	SOGNDAL - SELSENG	NO	+61:20:04	+06:56:00	421	P
2700	STADLANDET	NO	+62:08:52	+05:12:50	75	P
2701	VIK I SOGN III	NO	+61:04:22	+06:34:53	65	P
2702	YTRE SOLUND	NO	+61:00:16	+04:40:32	3	P
2703	ANDALSNES	NO	+62:33:56	+07:40:37	20	P
2704	EIDE PA NORDMORE	NO	+62:53:29	+07:23:26	49	P
2705	HALSAFJORD II	NO	+62:58:33	+08:14:34	12	P

2706	HUSTADVATN	NO	+62:54:32	+07:14:43	80	P
2707	NORDDAL	NO	+62:14:52	+07:14:29	28	P
2708	OKSENDAL	NO	+62:41:08	+08:25:27	47	P
2709	ORSKOG	NO	+62:28:44	+06:49:12	4	P
2710	RINDAL	NO	+63:02:17	+09:13:14	228	P
2711	SUNNDALSORA III	NO	+62:40:30	+08:33:32	6	P
2712	SURNADAL	NO	+63:00:18	+09:00:41	39	P
2713	VERMA	NO	+62:20:30	+08:03:06	247	P
2714	AUNET	NO	+63:03:21	+11:34:09	302	P
2715	AURSUND	NO	+62:40:26	+11:27:15	685	P
2716	BESSAKER	NO	+64:14:42	+10:19:40	12	P
2717	HITRA	NO	+63:37:24	+08:44:08	23	P
2718	SKJENALDFOSSEN I ORKDAL	NO	+63:17:42	+09:44:53	84	P
2719	SONGLI	NO	+63:19:48	+09:38:42	300	P
2721	BANGDALEN	NO	+64:19:54	+11:32:40	62	P
2722	HEGRA II	NO	+63:26:25	+11:15:23	33	P
2724	LIAFOSS	NO	+64:50:18	+11:57:24	44	P
2725	NAMDALSEID	NO	+64:15:02	+11:12:01	86	P
2728	OSTAS I HEGRA	NO	+63:29:15	+11:21:19	175	P
2729	SKJAEKERFOSSEN	NO	+63:50:21	+12:01:23	110	P
2730	SORLI	NO	+64:14:35	+13:46:14	370	P
2731	TUNNSJO	NO	+64:41:03	+13:39:24	376	P
2732	ALSVAG I VERSTERALEN II	NO	+68:54:52	+15:12:38	18	P
2733	BODOE - VAGONES	NO	+67:16:59	+14:28:00	33	TP
2735	LEIRFJORD	NO	+66:04:00	+12:54:56	53	P
2736	LEKNES I LOFOTEN	NO	+68:08:26	+13:36:34	13	P
2737	LUROY	NO	+66:23:22	+13:11:13	115	P
2738	OKSNINGOY	NO	+65:07:22	+12:22:24	17	P
2739	STEIGEN	NO	+67:55:18	+15:07:01	35	P
2740	SULITJELMA	NO	+67:08:04	+16:04:15	142	P
2741	SUSENDAL	NO	+65:21:30	+14:15:38	498	P
2742	TUSTERVATNET II	NO	+65:49:49	+13:54:24	439	P
2744	BONES I BARDU	NO	+68:38:44	+18:14:44	230	P
2745	DIVIDALEN	NO	+68:46:41	+19:42:36	228	TP
2748	SAETERMOEN II	NO	+68:51:38	+18:20:15	114	P
2749	STORSTEINNES I BALSFJORD	NO	+69:14:49	+19:13:51	27	P
2750	TORSVAG FYR	NO	+70:14:44	+19:30:02	21	TP
2752	KAUTOKEINO	NO	+68:59:48	+23:02:00	307	P
2753	KAUTOKEINO II	NO	+69:01:00	+23:02:02	330	P

6. Summary

Because of the ongoing global climate change, past observations give a potentially biased estimate of the present and near-future climate. This is not only the case for time mean conditions (e.g., the long-term mean temperature), but also for many other aspects of climate variability (e.g., the frequency of “very warm” months exceeding a given threshold temperature).

To make past observations representative of present or future climate conditions, they should be adjusted for the effects of climate change. In this report, we have attempted to do this by refining a method developed by Räisänen and Ruokolainen (2008a,b) to also include some information from high-resolution regional climate model simulations. The results have been presented in the form of maps and other diagrams. In addition, a set of detailed tables representing the probability distributions of interannual temperature and precipitation variability at a large number of Nordic locations as a function of time have been prepared and made available on-line.

A key finding from this analysis and from earlier studies is the higher signal-to-noise ratio of temperature than precipitation changes. Already in the present-day climate, about 70% of all months are expected to be warm (warmer than the median for 1961-1990) in northern Europe, and this fraction will increase as global warming proceeds. By contrast, the main uncertainty in estimating present-day precipitation climate is most likely sampling variability, rather than the effects of anthropogenic climate change. The latter will grow gradually greater with time, but even in the middle of this century, only about 60% of all months are projected to have above-median precipitation in northern Europe (although with a larger dominance of wet months in winter than in summer). With stronger time averaging, the effects of natural variability are partly smoothed out and the impacts of climate change become relatively stronger. Thus, for example, the probability of observing a warm or a wet year at any given time in the future is larger than the probability for an individual month to be warm or wet.

In this report, we have not considered changes in extremes outside the central 5-95% range of the probability distributions. In general, however, the frequency of extremes is expected to be sensitive even to relatively small shifts in the distribution. The calculations of Räisänen and Ruokolainen (2008b) suggest that the warming observed this far has already led to a dramatic increase in the probability of extremely high monthly (and seasonal-to-annual) mean temperatures. For example, the new monthly mean temperature records observed in Helsinki in December 2006 and March 2007 were estimated to have a return period of several centuries when estimated directly from 20th century observations, whereas the corresponding estimates for the actual present-day climate were of the order of 60-80 years. Thus, for temperature extremes in particular, past observations alone do not provide sufficient guidance for the near future.

Appendix: details of methodology

A.1 Data sets

The method used in this report requires three types of data: (i) observations of the local climate, (ii) observed time series of the global mean temperature, and (iii) climate model simulations. The latter are used both for deriving the regression coefficients that link the local climate to the global mean temperature, and for extrapolating the global mean temperature beyond the period of available observations.

As for (i), our analysis for individual locations (including the on-line tables) is based on station observations available from the European Climate Assessment & Dataset (ECA&D) (Klein Tank et al. 2002) website (http://eca.knmi.nl/). In addition, two gridded datasets are used for presenting results in map format. For temperature (Section 3), the analysis of Haylock et al. (2008) is used, as this extends nearly to the present time. However, an inspection of the Haylock et al. precipitation data revealed quality problems in recent years – specifically, long periods with zero precipitation in areas where precipitation had definitely fallen during the period in question. Therefore, we used for Figs. 4.2-4.3 precipitation data from the CRU TS 2.1 analysis (Mitchell et al. 2004). This analysis is only available up to the year 2002. By contrast, the ECA&D station observations and the Haylock et al. temperature analysis extend to the year 2008, although the time series are not complete everywhere. Both gridded data sets are available in a regular 0.5°× 0.5° latitude-longitude grid[3].

As for (ii), the HadCRUT3 (Brohan et al. 2006) analysis of the global mean temperature is used. Up to the year 2003, changes in the 11-year running mean global mean temperature are obtained directly from this data set. After this, they are inferred from the Third Coupled Model Intercomparison Project (CMIP3) simulations described below.

As for (iii), the analysis is primarily built on the same 19 global climate model simulations from the CMIP3 intercomparison (Meehl et al. 2007) that were used in Räisänen and Ruosteenoja (2008). The simulations cover the 20th and 21st centuries, with greenhouse gas concentrations following the SRES A1B scenario after the year 2000. However, following Räisänen and Ruokolainen (2009), 13 RCM simulations from the ENSEMBLES (Hewitt and Griggs 2004) project are used to add fine-scale regional detail to the climate change estimates. This aspect is described in more depth in the next subsection.

[3] The Haylock et al. (2008) data set is also available in a 0.25° grid, but the additional value provided by the higher resolution was considered small in comparison with the required increase in computing time.

A.2 Derivation of regression coefficients

In Räisänen and Ruokolainen (2008a,b), the regression coefficients that relate the local climate to the global mean temperature were derived from the CMIP3 GCM simulations for the SRES A1B emission scenario. The CMIP3 data set has two advantages for this purpose: simulations are available for a large number of quasi-independent models, and their length (years 1901-2098) and the large global mean temperature change simulated during this period allow the regression coefficients to be estimated with relatively little sampling noise.

On the other hand, the coarse (typically ~300 km) resolution of the CMIP3 models makes them unable to simulate small-scale variations of climate change. Thus, Räisänen and Ruokolainen (2009) developed a method for combining the large-scale information from the CMIP3 simulations with regional detail from the ENSEMBLES RCMs, which have a much higher resolution (~25 km). They found the RCM information to have a relatively modest effect on the resulting climate change projections, but some details such as land-sea contrasts in warming became sharper and more physically plausible.

The limitations of the ENSEMBLES data set (e.g., the relatively small number of truly independent simulations and the short duration of some of them) make it difficult to use these simulations in a consistent manner in the extrapolation method of Räisänen and Ruokolainen (2008a,b). Therefore, we only use them to make a first-order adjustment to the regression coefficient for time mean climate. Denoting the CMIP3-based regression coefficients for time mean climate (in °C/°C for temperature and %/°C for precipitation) as B_{CMIP3}, the regression coefficients used here are calculated as

$$B = B_{CMIP3} + \Delta B \qquad \text{(A2.1)}$$

Here ΔB is the RCM effect on the best-estimate time mean climate change from 1961-1990 to 2021-2050 as determined by the method of Räisänen and Ruokolainen (2009) (the column "Combined-CMIP3" in their Figs. 4.1 and 4.3) divided by the CMIP3 19-model global mean temperature change (1.35°C) between the same two periods. By contrast, the coefficients describing the changes in interannual variability (standard deviation of temperature and coefficient of variation of precipitation) are inferred directly from the CMIP3 simulations. Because of the relatively low signal-to-noise ratio involved, the use of RCM data for refining the CMIP3-based estimates of the variability change was considered too uncertain. In practice, the precise method of treating the variability should not be very important, because the results discussed in this report are dominated by the changes in time mean climate, with changes in variability playing a secondary role.

The resulting best-estimate regression coefficients for January and July are shown in Figs. A2.1 (temperature) and A2.2 (precipitation). The coefficients for time mean temperature change suggest a strong warming in northern Europe in winter (more than 2°C per 1°C of global warming in Finland and northern Scandinavia) and a more moderate warming (about the same as the global mean temperature increase) in summer. Less warming is to be expected over Iceland than the rest of the Nordic area, and the impact of the land-sea distribution is seen as relatively sharp gradients along coastlines. The regression also suggests a general decrease in interannual temperature variability in winter, whereas the variability of summer temperatures is projected to remain nearly unchanged in northern Europe (lower part of Fig. A2.1).

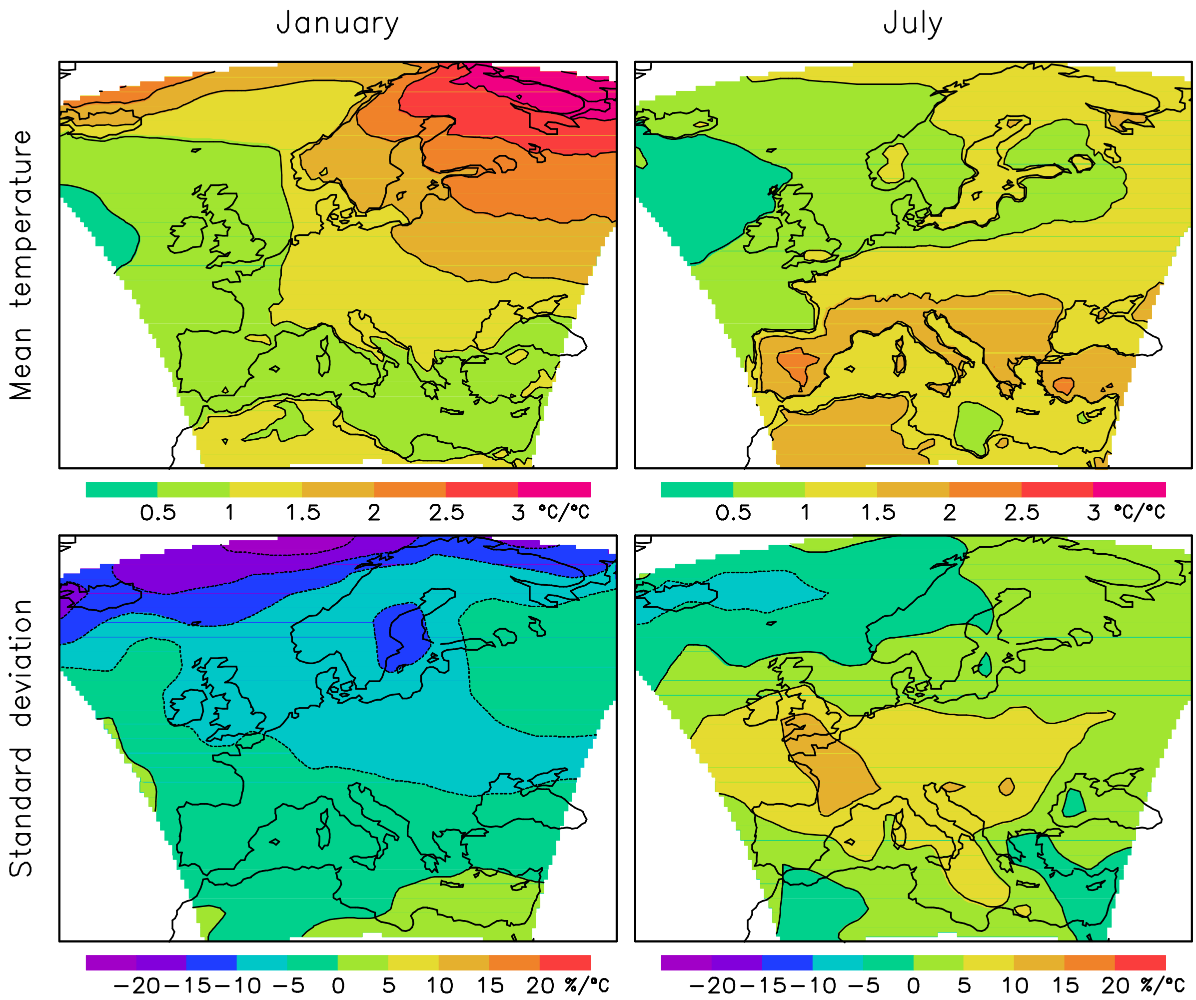

Figure A2.1. *Best-etimate regression coefficients giving the changes in local January (left) and July (right) mean temperature (above, unit °C/°C) and the interannual standard deviation of temperature (below, unit %/°C) per 1°C of global mean temperature change.*

The regression coeffcients for time mean precipitation (top of Fig. A2.2) exhibit a more noisy pattern, but suggest an increase in precipitation (locally up to over 10% per 1°C of global mean warming) in the whole Nordic area in winter. The changes in summer precipitation are projected to be smaller, with a borderline between increasing and decreasing precipitation in southwestern Scandinavia. The interannual coefficient of variation of precipitation (i.e., standard deviation / mean) is projected to remain nearly unchanged in the Nordic area, although there is a slight tendency towards higher values in summer. Thus, the interannual standard deviation of precipitation is expected to change broadly in proportion with the time mean precipitation.

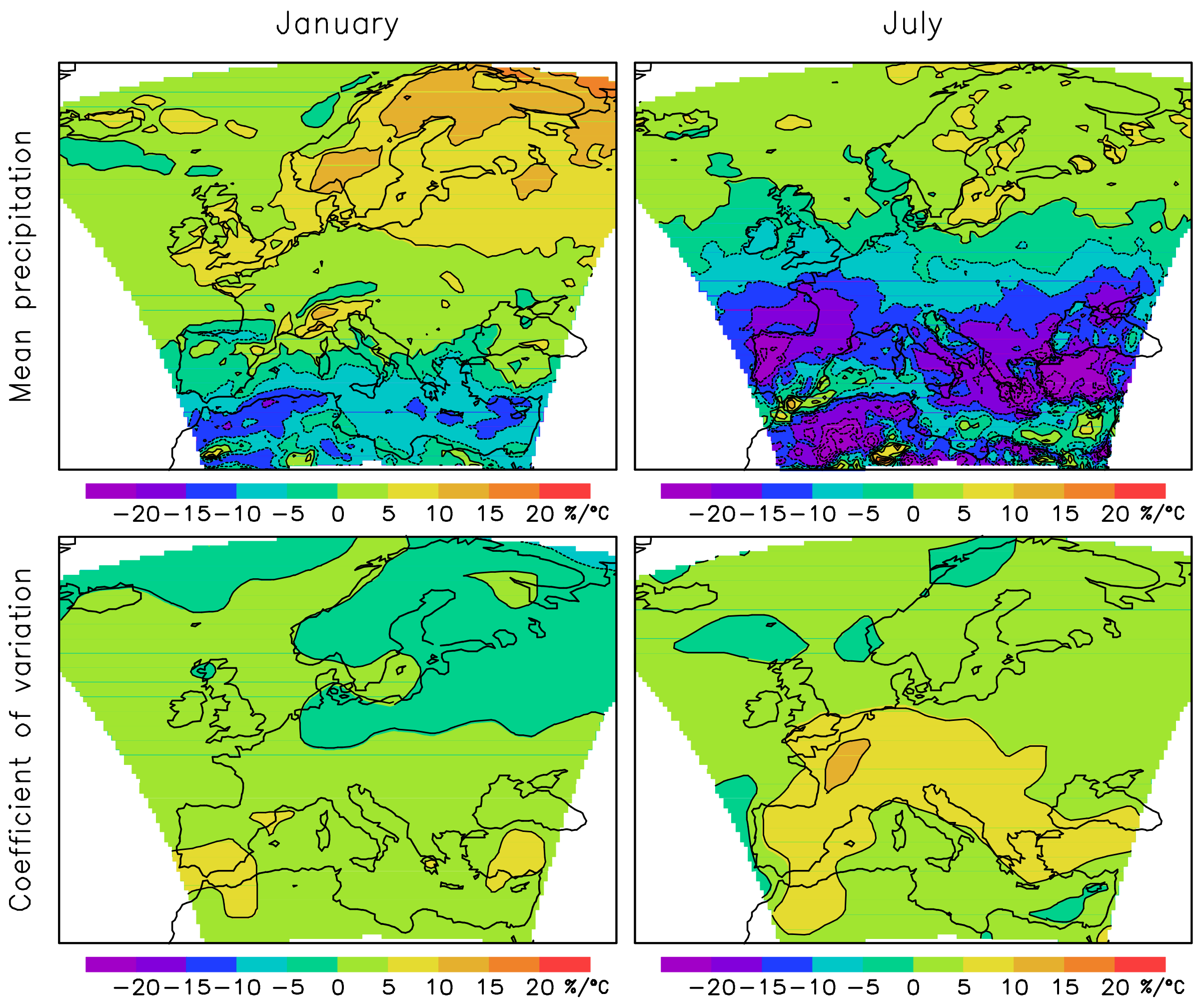

Figure A2.2. *Best-etimate regression coefficients giving the relative changes in local January (left) and July (right) mean precipitation (above, unit %/°C) and its interannual coefficient of variation (below, same unit) per 1°C of global mean temperature change.*

All the regression coefficients vary between the 19 CMIP3 models. As shown by Figs. 1.1 and 2.1, this introduces an uncertainty to how much past observations should be modified to take into account past and future changes in the global mean temperature. For the sake of brevity, however, we focus on best (i.e., multi-model mean) estimates of climate change in this report.

A.3 Smoothing of the probability distributions

The discrete frequency distributions obtained from the original or extrapolated observations were converted to continuous probability distributions using Gaussian kernel smoothing. The degree of smoothing is determined by a smoothing a parameter (*b* in Eq. (10) of Räisänen and Ruokolainen 2008a). For $b = 1$, the kernel returns a normal distribution with the same mean and standard deviation as the (original or extrapolated) observations. For smaller values of *b*, the mean and the standard deviation are the same, but the shape of the distribution follows the original discrete distribution more closely. With increasing *b*, sampling errors in the smoothed distribution decrease. On the other hand, too strong smoothing may introduce systematic biases in the smoothed distribution, particularly near its tails, if the distribution of the input data differs significantly from normal.

As shown by Räisänen and Ruokolainen (2008b), return period estimates in the extreme tails of the distribution may be strongly sensitive to the choice of the smoothing parameter. In this report we focus on the inner part of the distributions (between the 5th and 95th percentiles), where the sensitivity is much lower. Here we have chosen a higher value ($b = 1/2$) than that used by Räisänen and Ruokolainen (2008b) ($b = 1/3$), both because the baseline period is shorter and because the focus is not in the extremes, for which the systematic errors caused by excessive smoothing would be a larger issue.

The risk of systematic errors in the Gaussian kernel smoothing is smallest when the observations are nearly normally distributed. This condition holds generally less well for precipitation than for temperature, because the distribution of monthly precipitation totals tends to be positively skewed. To reduce or eliminate this skewness, the smoothing was applied to the square root of precipitation, rather than to precipitation itself.

Acknowledgments

We acknowledge the modeling groups, the Program for Climate Model Diagnosis and Intercomparison (PCMDI) and the WCRP's Working Group on Coupled Modelling (WGCM) for their roles in making available the WCRP CMIP3 multi-model dataset. Support of this dataset is provided by the Office of Science, U.S. Department of Energy. The ENSEMBLES data used in this work was funded by the EU FP6 Integrated Project ENSEMBLES (Contract number 505539) whose support is gratefully acknowledged.

References

Brohan, P., J.J. Kennedy, I. Harris, S.F.B. Tett and P.D. Jones, 2006: Uncertainty estimates in regional and global observed temperature changes: a new dataset from 1850. *Journal of Geophysical Research*, **111**, D12106, doi:10.1029/2005JD006548.

Haylock, M.R., N. Hofstra, A.M.G. Klein Tank, E.J. Klok, P.D. Jones, P.D. and M. New, 2008: A European daily high-resolution gridded data set of surface temperature and precipitation for 1950-2006. *Journal of Geophysical Research*, **113**, D20119, doi:10.1029/2008JD010201.

Hegerl G.C., F.W. Zwiers, P. Braconnot, N.P. Gillett, Y. Luo, J.A. Marengo Orsini, N. Nicholls, J.E. Penner and P.A. Stott, 2007: Understanding and Attributing Climate Change. Climate Change 2007: the Physical Science Basis, S Solomon et al., Eds., Cambridge University Press, pp 663-745.

Hewitt, C.D and Griggs, D.J. 2004: Ensembles-based predictions of climate changes and their impacts. *Eos*, **85**, 566.

Klein Tank, A.M.G. and Coauthors, 2002: Daily dataset of 20th-century surface air temperature and precipitation series for the European Climate Assessment. *Int. J. Climatol.*, **22**, 1441-1453.

Meehl, G.A., C. Covey, T. Delworth, M. Latif, B. McAvaney, J.F.B. Mitchell, R.J. Stouffer and K.E. Taylor 2007: The WCRP CMIP3 Multimodel Dataset: A New Era in Climate Change Research. *Bulletin of the Americal Meteorological Society*, **88**, 1383-1394.

Mitchell, T.D., T.R. Carter, P.D. Jones, M. Hulme and M. New 2004: A comprehensive set of high-resolution grids of monthly climate for Europe and the globe: the observed record (1901-2000) and 16 scenarios (2001-2100).Tyndall Centre Working Paper 55, 30 pp.

Nakićenović, N. and R. Swart (Eds.) 2000: *Emission Scenarios. A Special Report of Working Group III of the Intergovernmental Panel on Climate Change*. Cambridge University Press, 599 pp.

Räisänen, J. and L. Ruokolainen, 2006: Probabilistic forecasts of near-term climate change based on a resampling ensemble technique. *Tellus*, **58A**, 461-472.

Räisänen, J. and L. Ruokolainen, 2008a: Estimating present climate in a warming world: a model-based approach. *Climate Dynamics*, **31**, 573-585.

Räisänen, J. and L. Ruokolainen, 2008b: Ongoing global warming and local warm extremes: a case study of winter 2006-2007 in Helsinki, Finland. *Geophysica*, **44**, 45-65.

Räisänen, J. and L. Ruokolainen, 2009: Probabilistic forecasts of temperature and precipitation change by combining results from global and regional climate models, 36 pp. Available from http://www.atm.helsinki.fi/~jaraisan/CES_D2.3/CES_D2.3.html.

Räisänen, J. and K. Ruosteenoja, 2008: Probabilistic forecasts of temperature and precipitation change based on global climate model simulations, 46 pp. Available from http://www.atm.helsinki.fi/~jaraisan/CES_D2.2/CES_D2.2.html.

World Meteorological Organization (WMO), 1989: Calculation of Monthly and Annual 30-year Standard Normals. WMO-TD/NO. 341, Geneva, Switzerland, 11 pp.